Biogeochemistry
https://doi.org/10.1007/s10533-022-00925-9

Fingerprinting the elemental composition and chemodiversity of vegetation leachates: consequences for dissolved organic matter dynamics in Arctic environments

Alienor Allain · Marie A. Alexis · Maxime C. Bridoux · Guillaume Humbert · Yannick Agnan · Maryse Rouelle

Received: 26 October 2021 / Accepted: 22 March 2022

Abstract Dissolved organic matter is a key compartment for biogeochemical cycles in the Arctic and Subarctic terrestrial environments. With changing vegetation ecosystems, the chemical composition of organic matter is expected to shift and thus, the most labile part of it, namely the extractable fraction. To this date, few studies have focused on the fingerprinting of DOM fraction from different primary sources, and even less on its potential repercussions on the environment. In this study, we jointly characterized the chemical composition of bulk and water-extractable organic matter (WEOM) from different vegetation species typical of Subarctic ecosystems. Through a multi-analyses approach, including elementary analysis, solid state ^{13}C nuclear magnetic resonance, UV and 3D fluorescence spectroscopy, and high-resolution mass spectrometry, our results highlighted that the quantity and composition of produced WEOM significantly differed between vegetation sources and specifically between plant functional types (PFT, e.g., lichens, graminoids, and trees and shrubs). The relevance of optical indices was questioned, and the use of several of them was discarded for unprocessed WEOM study. However, the DOM proxies (optical indices, molecular composition, and stoichiometry) enabled to conclude that the lichen WEOM was likely less degradable than vascular plants WEOM, and among the latter group, graminoids produced more degradable WEOM than trees and shrubs. This work reported specific organic fingerprints for the different PFT. Consequently, the ongoing changes of vegetation in Arctic and Subarctic regions may greatly affect the composition of DOM that enters the soil and the hydrosystems, as well as the biogeochemical processes it is involved in.

Keywords Water extractable organic matter · Chemical characterization · Multi-analyses approach · Arctic ecosystem shift · Organic matter dynamics

Responsible Editor: Penny Johnes.

Supplementary Information The online version contains supplementary material available at https://doi.org/10.1007/s10533-022-00925-9.

A. Allain (✉) · M. A. Alexis · M. Rouelle
Sorbonne Université, CNRS, EPHE, UMR METIS, 75252 Paris, France
e-mail: alienor.allain@sorbonne-universite.fr

M. C. Bridoux
CEA/DAM Ile-de-France, Bruyères-le-Châtel, 91297 Arpajon, France

G. Humbert
Sorbonne Université, CNRS, INRAE, IRD, UPD, UPEC, Institute of Ecology and Environmental Sciences – Paris, iEES, 75005 Paris, France

Y. Agnan
Earth and Life Institute, Université Catholique de Louvain, 1348 Louvain-la-Neuve, Belgium

Published online: 29 April 2022

Introduction

Because of its high reactivity and mobility, dissolved organic matter (DOM) is considered to be an important fraction of soil organic matter (OM), at first as a key compartment of carbon dynamics (Bolan et al. 2011). DOM contains a complex and heterogeneous diversity of naturally occurring compounds involved in various important biogeochemical processes, such as metal complexation (Gangloff et al. 2014; Ren et al. 2015; Araújo et al. 2019), pollutant fate and transport (Schwarzenbach et al. 2016), and redox reactions. DOM also acts as a source of energy for the microbial community (Herbert and Bertsch 1995; Bowen et al. 2009) and plays a key role in nutrient cycling (Parker et al. 2015; Polishchuk et al. 2017). Its molecular composition in a given environment reflects its original source material but also the degradation processes (biotic and/or abiotic) it experienced (Wagner et al. 2015). Besides environmental parameters (temperature, precipitations, and soil properties such as pH, mineralogy, and moisture), the fate of DOM is related to its chemical composition. However, the identification of the factors controlling this composition and their implications on DOM quantity and properties in soils are still topical (Yates et al. 2016; Liu et al. 2021).

In terrestrial environments, vegetation is the primary source of DOM through processes of leaves throughfall, roots exudation, and litter dissolution. Degradation by microorganisms (i.e., bacteria and fungi) make then soil or aquatic DOM a mixture dominated by vegetation-derived molecules, and also composed of microbially-derived molecules (Gregorich et al. 2000; Nebbioso and Piccolo 2013). In the context of climate change and the related Arctic consequences (Arctic amplification, vegetation shifts, and permafrost thawing), large, changing, and growing terrestrial DOM fluxes are observed (Frey and Smith 2005; Olefeldt and Roulet 2012; Walvoord et al. 2012; O'Donnell et al. 2021). They appear to be a key component controlling biogeochemical cycles in the Arctic and subarctic regions (Fouché et al. 2017; McGovern et al. 2020; Pokrovsky et al. 2020; Beel et al. 2021), mainly because of the well-known high lability of DOM, that can lead to fast reprocessing of fresh leachates through microbial degradation (Osterholz et al. 2014; Johnston et al. 2019). The relatively low temperatures and related slow degradation processes, peculiar to Arctic ecosystems, strengthen the influence that the DOM produced by the initial vegetation leaching may have on such ecosystems. Indeed, several studies have highlighted the relationship between the initial vegetation leaching process and soil DOM chemical composition, microbial community composition and its metabolic activity, or greenhouse gas emission (Zak and Kling 2006; Hodgkins et al. 2016; Nielsen et al. 2017; Jassey et al. 2018). Besides, different types of vegetation proved to impact processes in soil, such as microbial activity and OM lability (Kiikkilä et al. 2005; Wickland et al. 2007; Lynch et al. 2019) whereas recent studies illustrated the influence of vegetation on DOM composition and export fluxes up to Arctic rivers (Kaiser et al. 2017) and marine environments (McGovern et al. 2020). However, among the numerous studies focusing on the chemical characterization of DOM in soils or in aquatic systems, only a few have characterized at the molecular level the primary DOM sources, namely fresh Arctic vegetation leachates.

The DOM includes a mixture of biochemical compounds (amino acids, sugars, vitamins, fatty acids), various complex biopolymers (proteins, polysaccharides, lignins), and very complex refractory degradation products. The very complex and diverse nature of organic compounds in DOM have pushed the limit of analytical techniques used to characterize them. The qualitative characterization of DOM in natural environments is usually based on different analytical techniques (Nebbioso and Piccolo 2013 and references therein; Minor et al. 2014 and references therein): mainly UV–Visible and fluorescence spectroscopy, solid or liquid state nuclear magnetic resonance (NMR), and/or, more recently, high resolution mass spectrometry (HRMS). Considering the limitation of each technique (Nebbioso and Piccolo 2013; Minor et al. 2014), the combination of several of them is generally recommended to allow comprehensive and meaningful characterization of DOM components (Minor et al. 2014; Rosario-Ortiz and Korak 2017). Indeed, the optical features (Fellman et al. 2010; Peacock et al. 2014) provide information on the relative contributions of different classes of compounds to DOM (aromatic, tyrosine-like, tryptophane-like, protein-like, humic-like). These techniques enable to ultimately hypothesize the origins of DOM (terrestrial vs. aquatic, freshwater vs. marine water, higher plant-derived vs. microbially

processed), but they only detect the colored DOM fraction able of absorption and fluorescence. In contrast, nuclear magnetic resonance (NMR) brings information on the entire DOM pool, but at the functional group scale. More recently, HRMS has emerged as a powerful tool for the analysis of extremely complex mixtures, such as water and soil-derived organic substances. It results in rapid and accurate interpretation of the elemental compositions of complex samples and has improved our understanding of the nature and molecular structure of DOM constituents (Zark and Dittmar 2018). Despite its limitation and selectivity towards compounds, it has showed to be a suitable technique for the investigation of very subtle biogeochemical processing of bulk DOM (Maria et al. 2019; Roth et al. 2019; Pan et al. 2020). HRMS offers an explicit way to describe and compare DOM samples (Alvarez-Rivera et al. 2019; Maria et al. 2019; Roth et al. 2019; Pan et al. 2020), due to its high resolution and mass accuracy that enable to assign unequivocal molecular formulae to a detected compound (Nebbioso and Piccolo 2013; Minor et al. 2014).

In this work, DOM produced by various vegetation sources was chemically characterized, in order to: (1) fingerprint Arctic vegetation leachates; (2) determine if the DOM produced by different vegetation are homogeneous or specific to the sources; (3) foresee its pathway in the environment based on the vegetation composition; and (4) hypothesize the potential consequences for Arctic environments and their study. To do so, we used a combination of analytical techniques for tracing the chemodiversity of Arctic vegetation leachates. The present multi-analysis study focuses on the simultaneous characterization of vegetation OM and corresponding water-extractable OM (WEOM) fraction, a proxy of DOM (Guigue et al. 2014). We determined the elemental composition (C, N), contributions of functional groups through solid state ^{13}C NMR, optical properties through UV–Visible spectrophotometry and excitation-emission matrix (EEM) fluorescence spectroscopy, and molecular composition through Orbitrap HRMS characterization of solid phase extracted WEOM ($WEOM_{SPE}$). Based on chemical composition, we discuss the implications for the DOM dynamics in Arctic environments and the use of DOM indices classically used in soils and aquatic environments.

Material and methods

Study site and vegetation sampling

Six vegetation species typical of four Arctic ecological habitats were sampled around Abisko Scientific Research Station (68° 21′ 16.1″ N 18° 48′ 57.7″ E) in Northern Sweden in June 2016 (early Summer) and September 2020 (late Summer) (Table 1). The four sites were located 975 m a.s.l. and 383 m a.s.l. on the east slope of Njulla Mountain, 599 m a.s.l. on the north-west slope of Baddosdievvá Mountain, and 361 m a.s.l. on the south shore of Lake Torneträsk. To each sampling site corresponded an ecological habitat: moss and lichen tundra, broadleaf forest, shrub tundra, and peatland respectively (Fig. 1). Each sampling site was composed of 1 to 3 plots of 900 m^2. On each plot, dominant vegetation species were identified, and those that might be sensitive to climate change (e.g., vegetation shift) were sampled: *Cladonia stellaris*, *Flavocetraria nivalis*, and *Betula nana* for shrub tundra, *C. stellaris* and *F. nivalis* for moss and lichen tundra, *Eriophorum vaginatum* for peatland, *B. pubescens* and *Salix* sp. for broadleaf forest. For each sampled vegetation species, the aboveground biomass that integrates soils annually was collected (e.g. hole vegetation of *C. stellaris* and *F. nivalis*, stem of *E. vaginatum*, and leaves of *B. nana*, *B. pubescens*, and *Salix* sp., see Table 1) on several individuals, and pooled to form composite samples. One to five sample replication was performed for each species/season combination (i.e., 7 combinations described from 21 composite samples). Plant functional types (PFT; namely lichen, graminoids, deciduous shrub, and deciduous tree) and plant physiology (vascular plants vs. lichens) were also determined for each species.

Sample preparation

The samples were oven dried (< 40 °C) for several days, then preserved in a dry place, at room temperature and protected from light (Fig. 1). Each composite sample was subsampled and considered for the characterization of (1) vegetation solid samples, and (2) WEOM samples. One set of those subsamples was ground using a rotor mill for vegetation (Ultra Centrifugal Mill ZM 200, Retsch, Haan, Germany) with a 6-tooth rotor and a 0.250 mm trapezoid holes sieve

Table 1 Number of field replicates, biological (plant functional types, physiology, organ sampled and stage of development) and environmental (sampling season and ecological habitat) characteristics of samples

Species	Season/species category	Field replicates n =	Plant functional types[a]	Physiology	Organ sampled	Stage of development	Sampling season	Ecological habitat[a]
C. stellaris	*C. stellaris*	3	Lichen	–	Entire vegetation	–	Early summer	Shrub tundra
		2	Lichen	–	Entire vegetation	–	Early summer	Moss and lichen tundra
F. nivalis	*F. nivalis*	1	Lichen	–	Entire vegetation	–	Early summer	Shrub tundra
		1	Lichen	–	Entire vegetation	–	Early summer	Moss and lichen tundra
		1	Lichen	–	Entire vegetation	–	Early summer	Peatland
E. vaginatum	*E. vaginatum* (Jun.)	1	Graminoids	Vascular	Stem	Intermediate	Early summer	Peatland
	E. vaginatum (Sep.)	3	Graminoids	Vascular	Stem	Mature	Late summer	Peatland
B. nana	*B. nana*	3	Deciduous shrub	Vascular	Mature leaf	Mature	Early summer	Shrub tundra
B. pubescens	*B. pubescens*	3	Deciduous tree	Vascular	Bud leaf	Young	Early summer	Broadleaf forest
Salix sp.	*Salix* sp.	3	Deciduous tree	Vascular	Bud leaf	Young	Early summer	Broadleaf forest

[a]Agnan et al. (2019) based on Walker (2000)

at 14,000 rpm. Those ground samples were referred as "vegetation OM" samples in this manuscript, and were used for elemental and solid-state ^{13}C NMR analyses.

The second set of those subsamples, different from the subsample previously ground, was extracted with ultrapure water (18 MΩ cm, PURELAB® Ultra, ELGA LabWater, United Kingdom), respecting a 1:100 (w:w) ratio on a dry weight basis, and shaken in pre-rinsed metal-free polypropylene centrifuge tubes and polyethylene flat caps for 2 h in a rotary shaker (Reax 2, Heidolph Instruments GmbH & CO, Schwabach, Germany) at 20 °C (number of samples and replicates per analytical method is specified in the corresponding paragraphs and in Fig. 1). Extracts were filtered through pre-rinsed nylon syringe filters (0.45 µm) and the obtained WEOM fractions were stored at < 4 °C until analysis. Those WEOM fractions were directly used for elemental, optical, and Orbitrap analyses. Part of the WEOM fraction was frozen at − 20 °C then freeze-dried (Cosmos freeze drier, Cryotec©, France), until vacuum reached 5 × 10 mTorr prior NMR analysis (Fig. 1).

One WEOM sample per category (i.e., 7 samples) underwent a solid-phase extraction (SPE) on strata-X (Phenomenex© Inc., CA, USA) cartridges (500 mg of sorbent). Prior to the SPE extraction, cartridges were conditioned with consecutive application of 3 mL isopropanol, 6 mL acetonitrile, 6 mL methanol containing 0.1% of formic acid and 6 mL of ultrapure water containing 0.1% formic acid. Then, approximately 10 mL of WEOM, with pH adjusted at 4.5 using concentrated formic acid, was applied at the rate of 1 mL min^{-1} to the cartridge. The cartridges were then rinsed with 4 mL acidified ultrapure water to remove the inorganic salts remaining in the dead volume of the cartridge; these salts could significantly reduce the sensitivity in electrospray ionization (ESI) analysis. Cartridges were subsequently dried and the analytes were eluted with 2.0 mL of acetonitrile/methanol/water (45/45/10) at pH 10.4. The eluted samples were then diluted 50:50 (v:v) with ultrapure water and

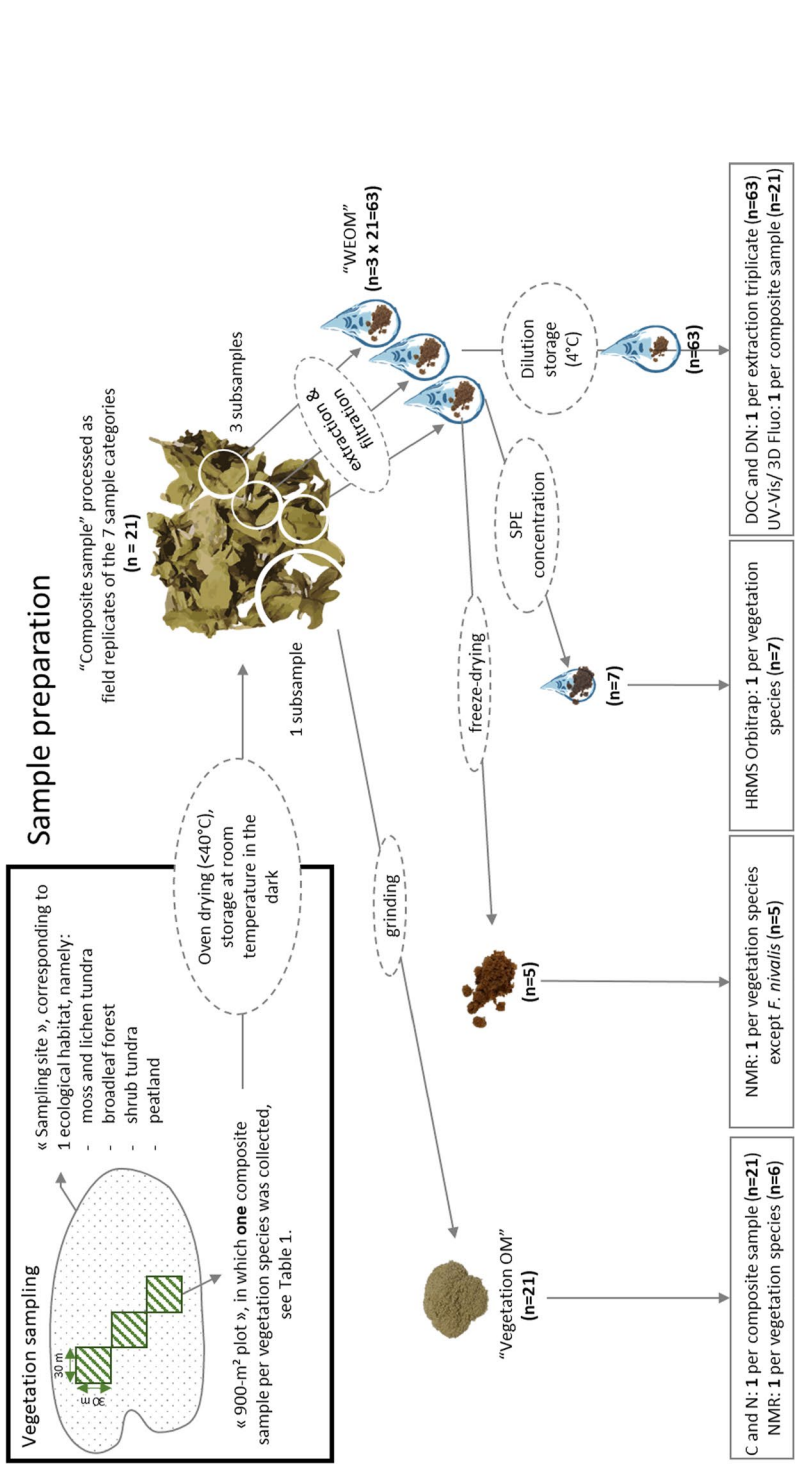

Fig. 1 Sampling protocol and sample preparation method, summarized for each analyze. The terms used in the manuscript ('sampling site', 'plot', 'composite sample', 'subsample', 'replicates') the type (ground or WEOM) and number ('n') of samples and replicates are detailed for each feature method

analyzed right away. Because low molecular weight compounds (< 100 Da) are expected to be lost in the rinsing and drying steps of the solid-phase extraction (Zhao et al. 2013), HRMS sample are here designated as $WEOM_{SPE}$.

Chemical analyses

Elemental analyses

The C and N content of vegetation OM were assessed on the 21 ground composite samples using an elemental analyser Pyro cube EA (Elementar, Hanau, Germany). Tyrosine was used as analytical standard.

Dissolved organic carbon (DOC) and dissolved nitrogen (DN) of WEOM, determined as non-purgeable organic carbon (NPOC) and total nitrogen (TN), respectively, were assessed using a TOC-L analyser (Shimadzu, Kyoto, Japan). Each of the 21 composite samples was extracted 3 times (extraction triplicates), one extraction blank was made for each extraction batch and samples were kept in the fridge (< 4 °C) before the analysis. WEOM samples were diluted 100 times with ultrapure water before analysis and C (TOC standard 25 mg L^{-1}, Sigma-Aldrich, Saint Louis, Missouri, United States) and N (1 mg L^{-1} N in H_2O, Merck Group, Darmstadt, Germany) standards were used as references. Limits of detection and quantification were calculated based on the analysis of 10 extraction blanks: 0.14 mg L^{-1} and 0.24 mg L^{-1}, respectively, for NPOC, and 0.03 mg L^{-1} and 0.07 mg L^{-1}, respectively, for TN.

Solid-state ^{13}C NMR

NMR analysis were performed with an Avance 500 MHz NMR spectrometer (Bruker, United States), operating at 125.8 MHz on ^{13}C, and calibrated with adamantane. Samples were packed in 4-mm zirconium rotors with Kel-F caps. Cross-polarization and magic angle spinning (CP–MAS) were applied with a spinning speed of 14 kHz. One vegetation OM sample of each category (i.e., 7 samples) was analysed. When allowed by the quantity of OC (namely for WEOM extracted from *C. stellaris*, *E. vaginatum* (Jun.), *B. nana*, *B. pubescens*, and *Salix* sp.), WEOM was also characterized through ^{13}C NMR (i.e., 5 samples), using inserts when material could not fill an entire rotor. Samples were analysed for a period of 2 to 16 h depending on the intensity of the obtained signal to optimize the signal to noise ratio (spin rate of 14,000 Hz, contact time of 10^{-3} s, recycle time of 2 s). Between 3128 and 112,640 scans were accumulated to obtain spectra. The line broadening parameter was 30. Between 10 and 30 peaks were identified for each spectrum.

Optical spectroscopy analyses

The WEOM of each field replicate (i.e., 21 samples) was characterized using ultraviolet and visible light absorbance (UV–Vis), and excitation-emission matrix (EEM) fluorescence. Samples were diluted between 3 and 100 times with ultrapure water to reach a maximum 254 nm absorbance of 0.1 and avoid inner-filtering effect (Ohno 2002). Absorbance spectra were acquired in 1 cm quartz Suprasil® cuvettes using a double-beam Uvikon XS Secomam® spectrophotometer (Aqualabo®, Champigny-sur-Marne, France) at 1 nm interval from 210 to 700 nm (200 nm min^{-1}). Ultrapure water was used as the reference.

Fluorescence analysis was performed using an Aqualog-UV-800 scanning spectrofluorometer (Horiba Jobin–Yvon, Longjumeau, France). The EEMs were collected using a high CCD detector gain at approximately 0.58 nm intervals (1 pixel) at emission wavelengths between 250 and 800 nm and a double-grating monochromator at excitation wavelengths of 240–800 nm at 5 nm intervals. A blank EEM was acquired daily with ultra-pure water and subtracted from sample EEM spectra. All EEMs were normalized to Raman emission of ultrapure water and reported in Raman units (RU) and corrected for instrumental bias following the manufacturer's method and dilution. Fluorescence intensities were thus reported in Raman units (RU).

High resolution Orbitrap LTQ XL mass spectrometry analysis

HRMS Orbitrap was performed on 2 lichen and 5 vascular plant $WEOM_{SPE}$ samples. Samples were infused into an ESI source which is selective toward polar compounds (i.e., DOM molecules containing carboxylic acids and other polar functional groups) using the same parameters as described in Maria et al. (2019). Before acquisition, the instrument was first externally calibrated following the manufacturer's manual using

the manufacturer's mixture consisting of caffeine, MRFA (l-methionyl-arginyl-phenylalanyl-alanine acetate monohydrate), and ultramark 1621. During the acquisition, each individual spectrum was recalibrated online, using an internal lock mass consisting of a background ion previously identified by their isotopic distribution, mass accuracy, and MS/MS analysis. Typically, phthalates, such as di-2-ethylhexyl-phthalate (DEHP), at m/z 391 were used as a lock mass, and other identified background signals, such as dibutylphtalate (DBP) or polydimethylsiloxane (PDMS), were used to check the mass accuracy. Solvent blanks were run before and after each sample to clean up the ion source and to avoid cross-contamination and carryover from the precedent samples.

Data processing, and statistical analyses

Extractability

In this study, the extractability was defined as the proportion of C, N, or specific class of compounds included in the WEOM fraction in comparison with the vegetation OM.

To assess the extractable OC and N fraction of vegetation samples, the concentration of DOC and DN were normalized to the mass of vegetation dry matter (DM) and volume of water; the results were given in $mg_{DOC}\ g_{DM}^{-1}$ and $mg_{DN}\ g_{DM}^{-1}$ and were defined as the OC and N extractabilities. Values presented in this study correspond to the mean values of the extraction triplicates by n field replicates (Table 1; Fig. 1), and blank subtracted.

^{13}C-CP MAS NMR spectra integration

Peaks of NMR spectra were attributed based on Conte et al. (2010) and Kögel-Knabner (2002). For the vegetation OM samples, the spectrum integration was done through deconvolution using DMfit program (Massiot et al. 2002). Integration of the four main chemical shift regions was done according to Kögel-Knabner (1997, 2017), with alkyl-C ranging from 0 to 45 ppm, O-alkyl-C from 45 to 110 ppm, aromatic-C from 110 to 160 ppm, and carboxyl-C from 160 to 220 ppm. The relative contribution (in %) of each chemical shift region was determined by integrating and adding the areas of peaks whose maximum belongs to each region. For the WEOM samples, the very high hydrophilicity of samples seems to have induced atmospheric humidity uptake by freeze-dried WEOM. Similar behaviour was previously mentioned for DOM samples by Knicker (2011) and may have differently impacted the peak intensities. Consequently, we decided to report the spectra but not to take into account the relative contribution of the chemical regions for WEOM samples. We only commented the presence/absence of the peaks in the spectra for comparison with other analyses.

Optical indices

Most of the studies that developed optical indices were dedicated to marine or estuarine environment (Coble 2007). In this work, several of them were selected because they are supposed to reflect DOM properties that could be meaningful in terrestrial surface waters, like aromaticity, lignin content, humification degree, terrestrial vs. microbial origin, or molecular weight. Based on absorbance analysis, 5 indices were calculated to characterize WEOM (Table 2). Absorption coefficient at 350 nm (a_{350}) describes the content of lignin polyphenols in DOM; relatively higher values indicate more lignin phenol in a sample (Battin 1998; Garcia et al. 2018). Specific ultraviolet absorbance at 254 nm ($SUVA_{254}$) reflects the aromaticity of a sample (Weishaar et al. 2003). Samples with higher values of $SUVA_{254}$ are typically more aromatic. Absorption ratio at 254 nm to 365 nm (E2/E3) and slope ratio (S_R) both described the molecular weight; lower values indicate DOM with higher molecular weight (Guo and Chorover 2003; Hunt and Ohno 2007). S_R can also indicate DOM biodegradability; lower molecular weight compounds being biologically more stable (Fouché et al. 2020).

Based on fluorescence analysis, three indices were calculated to characterize DOM (Table 2). Fluorescence index (FI) describes the relative dominance of microbially vs. higher plants derived OM in a sample; higher values (greater than 1.9) indicate a preponderance of microbial DOM, and lower values (less than 1.3) indicate predominantly terrestrial plant sources (McKnight et al. 2001; Chen et al. 2003; Cory and McKnight 2005). The humification index (HIX) describes the condensation of DOM (Ohno 2002; Ohno and Bro 2006; Parot 2017); values range from 0 to 1, and higher values indicate more condensed DOM (i.e., with higher aromaticity and molecular

Table 2 Absorbance (a_{350}, $SUVA_{254}$, E2/E3 and S_R) and fluorescence (FI, HIX and BIX) indices used to characterize DOM, calculation and relationship between DOM characteristic and indices, and literature were they are described

Name	Abbreviation	Calculation	Relationship	Source(s)
Absorbance				
Absorption coefficient at 350 nm (L mg_C^{-1} m^{-1})	a_{350}	A_{350} * 2.303/r * [DOC]	Positively correlated with dissolved lignin phenols	Battin (1998) and Garcia et al. (2018)
Specific ultraviolet absorbance at 254 nm (L mg_C^{-1} m^{-1})	$SUVA_{254}$	A_{254} * 2.303/r * [DOC]	Positively correlated with aromaticity	Weishaar et al. (2003)
Absorption ratio at 254 nm to 365 nm	E2/E3	A_{254}/A_{365}	Negatively correlated with molecular weight	Guo and Chorover (2003) and Hunt and Ohno (2007)
Slope ratio	S_R	$S_{275\text{-}295}/S_{350\text{-}400}$	Negatively correlated with molecular weight	Helms et al. (2008)
Fluorescence				
Fluorescence index	FI	$I_{(370/450)}/I_{(370/500)}$	Positively correlated to the relative proportion of microbial derived vs. higher plant derived OM to the DOM pool	Chen et al. (2003), Cory and McKnight (2005) and McKnight et al. (2001)
Humification index	HIX	$I_{(254/435–480)}$ / $(I_{254/435–480} + I_{(254/300–345)})$	Positively correlated with humification and aromaticity	Ohno (2002), Ohno and Bro (2006) and Parot (2017)
Index of recent autochthonous contribution	BIX	$I_{(310/380)}/I_{(310/430)}$	Positively correlated to the relative proportion of autochthonous vs. terrestrial contribution to DOM	Huguet et al. (2009)

A_x and a_x refer to absorbance (m^{-1}) and absorption (L mgC^{-1} m^{-1}) coefficient at a given wavelength x, $S_{x\text{-}y}$ refers to spectral slope between x and y (m^{-1}), $I_{(x–y)}$ to fluorescence intensity at Ex/Em = x/y nm and r is the optical path length of the spectrometer cuvette

weight). The index of recent autochthonous contribution (BIX) characterizes fresh production of DOM linked to biological activity (Huguet et al. 2009); values of BIX discriminate low (< 0.5), intermediate (0.6–0.8) and strong autochthonous contribution from bacterial origin (> 0.8).

Fluorescence peak picking

The (Ex_{max}/Em_{max}) of local maximum fluorescence intensity were identified through peak picking. This visual inspection of the EEMs was preferred as the number of samples did not allow a robust model of the dataset using a parallel factor analyse (PARAFAC). The position (i.e., Ex_{max}/Em_{max}) of maximum fluorescence intensity of the EEMs were determined using a 2D representation of the fluorescence data, that covered tyrosine-like ($Ex_{max}/Em_{max} = 275/305$), tryptophane-like ($Ex_{max}/Em_{max} = 275/340$), and humic-like ($Ex_{max}/Em_{max} = 320–370/420–480$ and $Ex_{max}/Em_{max} = 230–260/380–480$) fluorescence peaks areas (Coble 1996; Fellman et al. 2010; Mann et al. 2016). For each Ex_{max} range (265–320 nm, and 300–400 nm), one or two maximum fluorescence intensity were identified, along with their matching Em_{max}.

HRMS Orbitrap data processing and data visualization

All data were acquired using the Thermo Xcalibur software. Before processing, mass accuracy was checked by the attribution of the elemental composition of known background compound that are phthalate and PDMS (error observed before recalibration systematically lower than 2 ppm). The post-acquisition recalibration was then based on a 5-order polynomial equation. A set of naturally occurring compounds previously identified in lignin, natural organic matter (NOM) and plants were selected to represent internal recalibrants over the mass range considered. The calibration was then validated by checking that the average error corresponding to reference masses was lower than 0.5 ppm. After background ion removal, the elemental compositions were assigned, with an error lower than 3 ppm. The elemental compositions authorized were $C_{1-70}H_{0-140}O_{1-25}$ with a user-defined mass tolerance of 3 ppm. The assignments were validated by checking the error distribution which has to be between -3 and 3 ppm, and equitably distributed around 0 ppm. After deisotoping and declustering, each compound was assigned a molecular formula. Due to the relatively low amount of nitrogen in the WEOM samples, nitrogen was excluded from the element list in the molecular assignment. Moreover, since the ionization yield may differ between molecules, the high-resolution data are not considered in a quantitative way, but to allow the qualitative comparison of molecules identified in the different species $WEOM_{SPE}$.

Based on the attributed formulas, Venn diagrams were assessed to display specific and common compounds detected in samples. Some regions of Venn diagrams were then plotted in Van Krevelen (VK) diagrams to display and summarize complex mass spectrometric data by sorting elemental formulas according to their elemental ratios (Kim et al. 2003). Indeed, VK diagrams represented the elemental H/C (y axis) versus X/C (x axis) ratios, where X is a heteroatom (i.e., oxygen, nitrogen…). In this study, O was selected as the heteroatom represented in the VK diagrams. The positioning of compounds within the VK diagram related WEOM composition to those of known biomolecules families present in these samples (lipid-like, protein-like, amino sugar and carbohydrate-like, unsaturated hydrocarbon-like, lignin-like, tannin-like and condensed aromatic structures, see SI1) (Grannas et al. 2006; Maria et al. 2019). Although the VK graphical representation of elemental formulas provided an overview of the compound categories, care was taken due to the overlap among different categories along both O/C and H/C axes.

Based on the information provided by HRMS Orbitrap, indices were calculated. The double bond equivalent (DBE_{AI}) and aromaticity index (AI) were calculated (based on Koch et Dittmar 2006) for each molecular compound. If the AI of a formula was negative, its value was considered as 0. Then, for one sample, molecular compounds were classified based on their AI values: compounds with AI = 0 were assigned to aliphatic compounds. Compounds with AI comprised between 0 and 0.5 were assigned to olefinic/alicyclic compounds (Maria et al. 2019). An AI value ranging between 0.5 and 0.67 indicates aromatic cores, possibly including heteroatoms. An AI value greater than 0.67 indicates condensed aromatic structure in the molecule. Then, for each sample, mean DBE_{AI}, mean AI, mean H/C, mean O/C

Table 3 C (%), N (%), DOC ($mg_{DOC}\ g_{DM}^{-1}$), DN ($mg_{DN}\ g_{DM}^{-1}$) values and C/N and DOC/DN ratio values of *C. stellaris*, *F. nivalis*, *E. vaginatum* (Jun.) and (Sep.), *B. nana*, *B. pubescens* and *Salix* sp

Sample category	Vegetation OM				WEOM			
		C (%)	N (%)	C/N		DOC ($mg_{DOC}\ g_{DM}^{-1}$)	DN ($mg_{DN}\ g_{DM}^{-1}$)	DOC/DN
	n	Mean ± s.d	Mean ± s.d	Mean ± s.d	n	Mean ± s.d	mean ± s.d	Mean ± s.d
Lichens								
C. stellaris	5	$42.3^{ac} \pm 0.3$	$0.5^{ab} \pm 0.1$	$86^{ab} \pm 10$	15	$11.8^{a} \pm 1.6$	$1.1^{ac} \pm 0.3$	$12^{a} \pm 3$
F. nivalis	3	$41.7^{a} \pm 0.3$	$0.5^{ab} \pm 0.1$	$94^{ab} \pm 19$	9	$14.1^{ab} \pm 1.0$	$1.2^{abc} \pm 0.3$	$13^{ac} \pm 2$
mean	**8**	**42.0***	**0.5***	**89***	**24**	**12.7***	**1.1**	**12***
s.d		**0.4**	**0.01**	**13**		**1.8**	**0.3**	**3**
Vascular plants								
E. vaginatum (Jun.)	1	44.5^{abc}	2.5^{abc}	18^{abc}	3	16.7^{abc}	4.8^{ab}	3^{a}
E. vaginatum (Sep.)	3	$44.6^{abc} \pm 0.2$	$0.4^{a} \pm 0.1$	$128^{a} \pm 20$	9	$9.7^{a} \pm 5.5$	$0.2^{c} \pm 0.2$	$53^{b} \pm 16$
B. nana	3	$48.8^{b} \pm 0.5$	$3.0^{bc} \pm 0.2$	$16^{bc} \pm 1$	9	$33.4^{abc} \pm 3.2$	$1.0^{ac} \pm 0.3$	$37^{bc} \pm 12$
B. pubescens	3	$46.3^{bc} \pm 0.2$	$3.4^{c} \pm 0.2$	$14^{c} \pm 1$	9	$50.0^{bc} \pm 8.5$	$4.1^{ab} \pm 0.7$	$13^{ac} \pm 1$
Salix sp.	3	$47.3^{b} \pm 0.6$	$4.3^{c} \pm 0.2$	$11^{c} \pm 1$	9	$73.8^{c} \pm 31.4$	$5.1^{b} \pm 2.1$	$15^{abc} \pm 1$
mean	**13**	**46.6***	**2.8***	**40***	**39**	**39.8***	**2.8**	**28***
s.d		**1.7**	**1.5**	**51**		**27.9**	**2.3**	**20**

Each value corresponds to the mean ± the standard deviation calculated for n field replicates of the same sample category. Additionally, the mean and standard deviation (s.d.) were calculated for lichens on one hand, and vascular plants on the other hand

[a,b,c]Indicate significant differences between species

*Indicates significant differences between vascular plants and lichens

were calculated, and the number of molecular compounds attributed to each biomolecular families were counted.

Data treatment

Statistical analyses were performed using R 3.6.1 (The R Foundation for Statistical Computing, Austria) and RStudio 1.2.1335 (RStudio Inc., MA, USA). Statistical significance was tested using non-parametric Mann–Whitney U test ($\alpha = 0.05$), and Kruskall-Wallis test ($\alpha = 0.05$) with a post-hoc Dunn test ($\alpha = 0.05$) using the "dunn.test" package (Dinno 2017). Mann–Whitney U test was performed to compare the medians of measured variables of vascular plants vs. lichens, whereas Kruskall-Wallis and Dunn tests were used to compare medians of measured variables of the 7 vegetation categories. These comparisons enable to discuss the influence of PFT, plant physiology (e.g., vascular plants vs. lichens), and species on the quantitative variables that characterise vegetation OM, and WEOM. Correlations between optical and molecular indices were tested with the

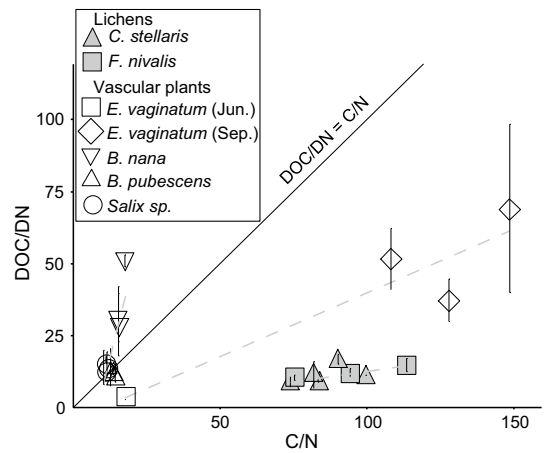

Fig. 2 C/N of vegetation OM samples versus DOC/DN of WEOM of *C. stellaris* (solid triangle), *F. nivalis* (solid square), *E. vaginatum* (Jun.) (blank square), *E. vaginatum* (Sep.) (blank diamond), *B. nana* (blank inverted triangle), *B. pubescens* (blank triangle), and *Salix* sp. (blank circle). Solid and blank symbols are related to lichens and vascular plants respectively. Each plot and error bar represent the mean and standard deviation of DOC/DN values calculated for extraction triplicates respectively. The black plain line equation is DOC/DN = C/N. The grey dotted lines correspond to extractability trends specific to each VFT

non-parametric Spearman test, using the "corrplot" package (Wei and Simko 2021).

Results

Carbon and Nitrogen composition of vegetation OM, and WEOM

Individual C and N contents of vegetation OM samples (Table 3) ranged between 41.4 and 49.3%, and between 0.3 and 4.5%, respectively, with C and N content being significantly greater in vascular plants compared to lichens. Individual C/N ratios varied from 10 to 149, with lichen C/N ratios significantly greater than vascular plant C/N ratios. It is noteworthy that *E. vaginatum* (Jun.) and (Sep.) had similar C content (44.5, and 44.6 ± 0.2%, respectively), but different N content (2.5 and 0.4%, respectively), and C/N ratio (18 and 128 respectively).

Individual OC and N extractability ("DOC" and "DN" respectively, Table 3) of vegetation samples ranged between 4.7 and 101.9 $mg_{DOC}\ g_{DM}^{-1}$, and 0.07 and 6.34 $mg_{DN}\ g_{DM}^{-1}$ respectively. The OC extractability was significantly higher for vascular plants (39.8 ± 27.9 $mg_{DOC}\ g_{DM}^{-1}$) compared to lichens (12.7 + 1.8 $mg_{DOC}\ g_{DM}^{-1}$), whereas no significant difference was detected between vascular plant, and lichen N extractabilities. Individual DOC/DN ratios ranged between 3 and 60 and appeared significantly higher for vascular plants compared to lichens.

Distinct relationships between the C/N and the DOC/DN values could be observed for the different species (Fig. 2): The C/N values were equal to DOC/DN values for *B. pubescens*, and *Salix* sp. respectively (Fig. 2: on the solid line, where DOC/DN = C/N). The C/N values were higher than DOC/DN for *C. stellaris*, *F. nivalis*, and *E. vaginatum* (Fig. 2: to the right of the solid line). On the other hand, C/N values were lower than DOC/DN for *B. nana vaginatum* (Fig. 2: to the left of the solid line).

NMR of vegetation OM samples

In the alkyl-C region, the peaks at 21, 25, 30, and 33 ppm, assigned to $–CH_3$ of acetyl groups and linear methylene chains of lipids, hemicellulose, cutin-like, and other aliphatic bio-moieties were observed in all samples (See Conte et al. 2010; Kögel-Knabner 2002 and references therein for peak attribution references). On the other hand, peaks at 37 and 42 ppm, attributed to lignin- and chlorophyll-like structures, respectively, were observed only in spectra of *B. nana* and *B. pubescens* samples (Fig. 3).

In the O-alkyl C region, resonances at 53 and 56 ppm due to methoxyl $–CH_2O–$ present in lignin-like and protein structures were only observed for *Salix* sp., *B. nana*, and *B. pubescens*. Peaks at 63–65 ppm were attributed to crystalline and amorphous cellulose and hemicellulose. Peaks at 72–75 ppm were attributed to cellulose, hemicellulose, and lignin. Peaks at 85–89 ppm were attributed to C4 of crystalline and amorphous cellulose. Peaks at 100 ppm and 105 ppm were attributed respectively to hemicellulose and cellobiose units of cellulose or syringyl unit C of lignin. This resonance at 63–65, 72–75, 85–89, 100, and 105 ppm were observed in all samples.

The chemical regions from 110 to 160 ppm was typically attributed to resonance of aromatic and phenolic C and was generally related to C in lignin molecules: resonance at 115 ppm and 131 ppm were both attributed to p-hydroxyphenyl C, whereas resonances at 144 and 155 were attributed to lignin guaiacyl and syringyl units and tannins. The signal in this region was observed for *B. nana*, *B. pubescens*, and *Salix* sp. bulk samples. Low signal intensity was observed for *E. vaginatum* sample compared to trees and shrub samples. Resonances due to *p*-hydroxyphenyl C were high in *Salix* sp., whereas resonance due to lignin guaiacyl, and syringyl units and tannins was mainly observed for *B. nana* and *B. pubescens*.

The only peak present in the carboxylic-C region (172 ppm) was due to aliphatic amide C from proteins or carboxylic C. It was present in all samples and the signal was less intense for *C. stellaris* and *F. nivalis* than *E. vaginatum*, *B. nana*, *B. pubescens*, and *Salix* sp.

The main relative contributor to NMR spectra of vegetation OM was the O-alkyl C region in all sample spectra: it represented 52 to 90% of the total signal of all vegetation OM samples (Table SI2). On the other hand, carbonyl C region was the less intense region, with only 2 to 8% of the total signal for the whole set of vegetation OM sample. The aromatic C region was null for *C. stellaris* and *F. nivalis*. It was only present

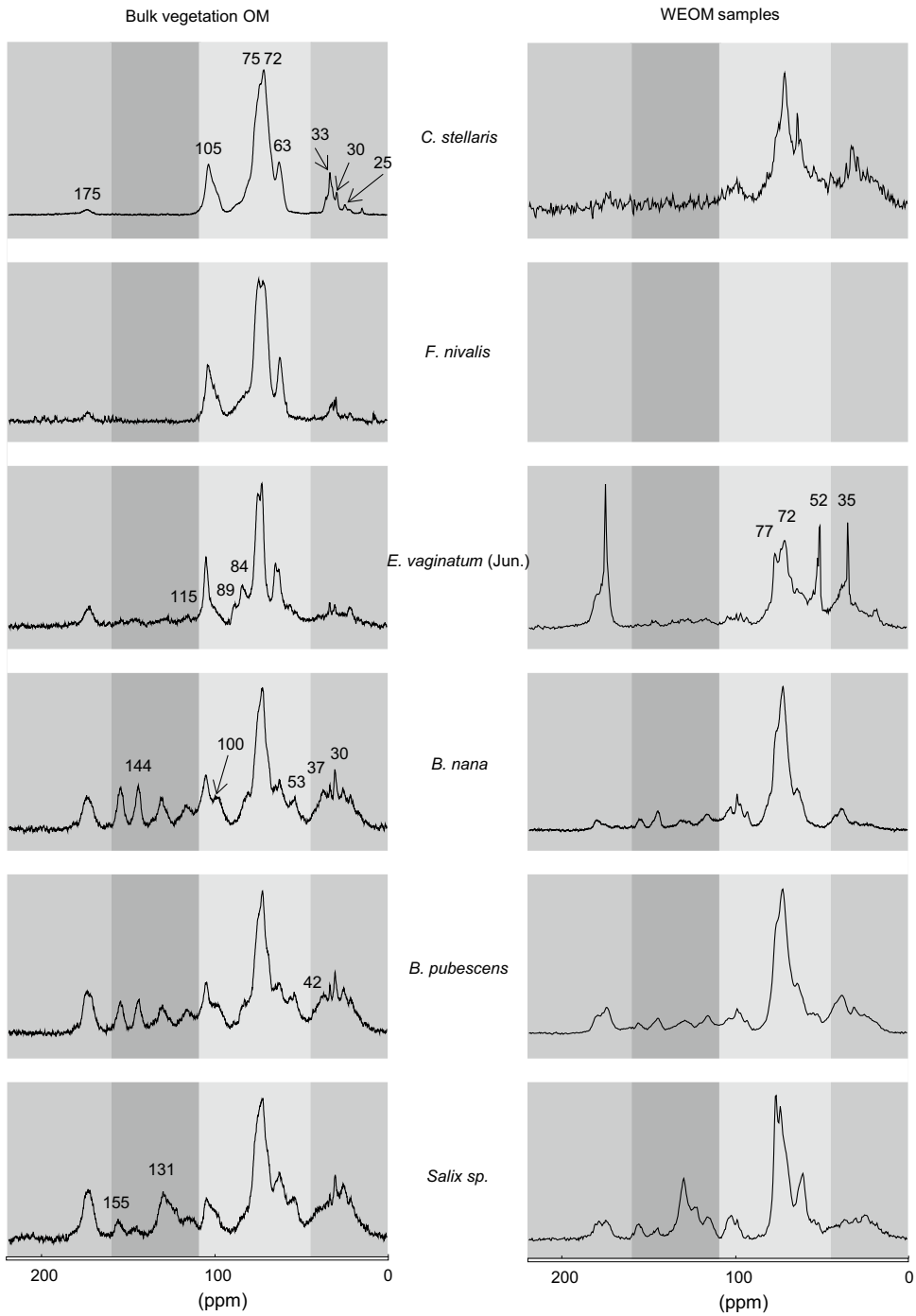

Fig. 3 Solid state CP-MAS ^{13}C-NMR spectra of bulk OM (left) and corresponding WEOM (on the right) samples of *C. stellaris*, *F. nivalis*, *E. vaginatum* (Jun.), *B. nana*, *B. pubescens* and *Salix* sp. Chemical shifts of interest, and chemical shift regions (in ppm) are reported on spectra. Because of low freeze-dried WEOM quantity and C concentration, no spectrum could be obtained for the WEOM of *F. nivalis*

Table 4 Absorbance (a_{350}, E2/E4, E2/E3, S_R and $SUVA_{254}$) and fluorescence (BIX, FI and HIX) indices values of WEOM samples

Sample category	n	Absorbance UV–Visible				Fluorescence		
		a_{350} (L mg_C^{-1} m^{-1})	$SUVA_{254}$ (L mg_C^{-1} m^{-1})	E2/E3	S_R	BIX	FI	HIX
Lichens								
C. stellaris	5	$0.19^{ac} \pm 0.06$	$0.30^{c} \pm 0.08$	$5.34^{a} \pm 0.85$	$0.48^{ab} \pm 0.20$	$0.67^{b} \pm 0.08$	$1.23^{ab} \pm 0.03$	$0.43^{a} \pm 0.10$
F. nivalis	3	$0.11^{a} \pm 0.05$	$0.20^{a} \pm 0.05$	$5.78^{a} \pm 0.95$	$1.10^{b} \pm 0.11$	$0.54^{ab} \pm 0.14$	$1.18^{ab} \pm 0.11$	$0.45^{a} \pm 0.10$
mean	**8**	**0.16***	**0.34***	**5.50***	**0.58**	**0.62**	**1.21**	**0.44***
s.d		**0.06**	**0.14**	**0.71**	**0.39**	**0.12**	**0.07**	**0.09**
Vascular plants								
E. vaginatum (Jun.)	1	0.81^{abc}	0.99^{ab}	4.37^{abc}	0.12^{a}	0.74^{ab}	1.60^{a}	0.35^{ab}
E. vaginatum (Sep.)	3	$0.56^{abc} \pm 0.27$	$0.83^{ab} \pm 0.44$	$4.87^{ab} \pm 0.53$	$0.51^{ab} \pm 0.32$	NA	NA	NA
B. nana	3	$1.54^{b} \pm 0.09$	$1.26^{b} \pm 0.05$	$2.75^{bc} \pm 0.25$	$0.29^{a} \pm 0.27$	$0.22^{a} \pm 0.06$	$1.21^{ab} \pm 0.04$	$0.10^{b} \pm 0.01$
B. pubescens	3	$2.34^{b} \pm 0.75$	$1.79^{b} \pm 0.46$	$2.40^{c} \pm 0.36$	$0.32^{a} \pm 0.22$	$0.71^{b} \pm 0.13$	$1.12^{b} \pm 0.16$	$0.16^{ab} \pm 0.01$
Salix sp.	3	$0.98^{bc} \pm 0.15$	$0.85^{ab} \pm 0.12$	$3.55^{bc} \pm 0.71$	$1.20^{b} \pm 0.03$	$0.21^{a} \pm 0.04$	$1.36^{ab} \pm 0.34$	$0.08^{b} \pm 0.05$
mean	**13**	**1.31***	**1.17***	**3.47***	**0.49**	**0.42**	**1.27**	**0.14***
s.d		**0.76**	**0.48**	**1.07**	**0.4**	**0.27**	**0.23**	**0.08**

[a,b,c]Indicate significant differences between species

*Indicates significant differences between vascular plants and lichens

in vascular plant bulk OM, however varied by a factor of almost 2 between *E. vaginatum* (Jun.) and other vascular plants. The alkyl C region was more than two times more intense for vascular plants (except *E. vaginatum* which is in between) compared to lichens spectra.

NMR of WEOM samples

In the alkyl C region, resonance at 19, 25 and 30 ppm were present in spectra of *C. stellaris*, *B. nana*, *B. pubescens* and *Salix* sp. WEOM samples (Fig. 3), corresponding to C of aliphatic chains and other non-specific bio-moieties. For the same samples, spectra showed signal at 64, 72, 83, and 105 ppm, corresponding to chemical shifts of C in crystalline and amorphous polysaccharides. Signal at 177 ppm, corresponding to C present in carboxyl groups or amid groups of proteins, were present in all WEOM spectra. This peak appeared thin and especially intense for *E. vaginatum* (Jun.) WEOM sample. Signal at 116, 130, 145, and 156 ppm that could mainly correspond to aromatic C in lignin was only observed in vascular plant WEOM spectra, except for *E. vaginatum*. In *E. vaginatum* WEOM, the intense signals at 35 ppm and 52 ppm correspond to ($–CH_2–$) and N bound C respectively.

UV–Vis absorbance

Absorbance indices mean values were summarized in Table 4: individual a_{350} (positively correlated with dissolved lignin phenols, Table 2) values ranged between 0.07 and 2.98 L mg_C^{-1} m^{-1}, and a_{350} was significantly higher for vascular plants compared to lichens. $SUVA_{254}$ (positively correlated with aromaticity, Table 2) ranged between 0.16 and 2.31 L mg_C^{-1} m^{-1} and was significantly higher for vascular plant compared to lichen WEOM. Individual E2/E3 (negatively correlated with molecular weight, Table 2) values ranged between 2.07 and 6.64 and values were significantly higher for lichen compared to vascular plant WEOM. S_R (negatively correlated with molecular weight, Table 2) values ranged between 0.10 and 1.22, but values were not significantly different between vascular plant and lichen WEOM.

It was noteworthy that within absorbance indices, a_{350} and $SUVA_{254}$ values of *B. nana*, and *B. pubescens* WEOM were higher whereas E2/E3 values were particularly low. Among other vascular plants, *E. vaginatum* (Sep.) and (Jun.) always seem to show the values the closest to lichens.

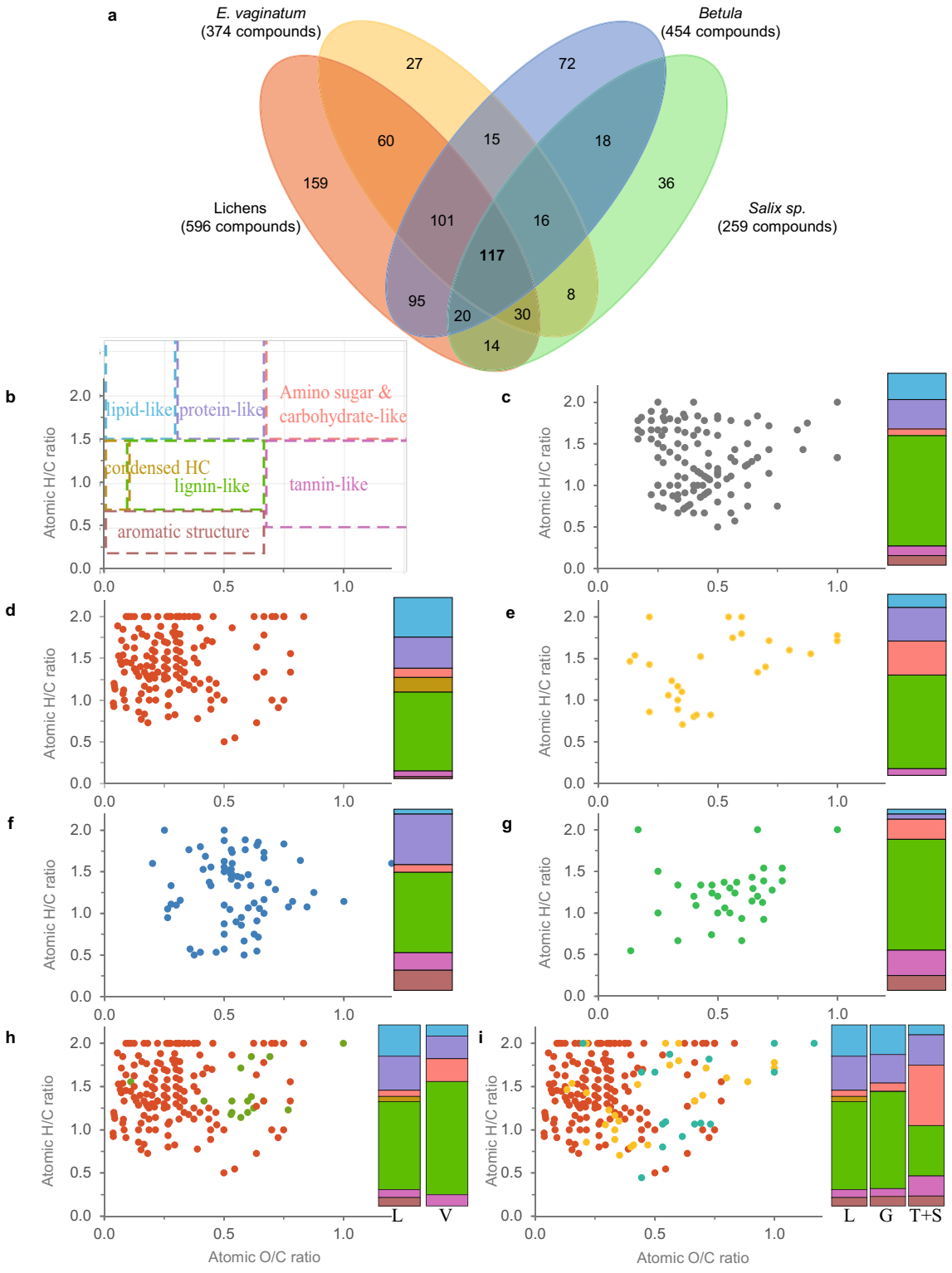
a
E. vaginatum
(374 compounds)
Betula
(454 compounds)
Lichens
(596 compounds)
Salix sp.
(259 compounds)
27
72
60
15
18
159
36
101
16
117
95
20
30
8
14
b
lipid-like
protein-like
Amino sugar &
carbohydrate-like
condensed HC
lignin-like
tannin-like
aromatic structure
Atomic H/C ratio
Atomic O/C ratio
c
d
e
f
g
h
i
L
V
G
T+S

◂**Fig. 4** **a** Venn diagram of common compounds to lichens (red), common compounds to *E. vaginatum* (yellow), common compounds to *Betula* (blue), and of *Salix* sp. (green) $WEOM_{SPE}$ samples, **b** VK diagram displaying compound classes commonly observed in natural environments. VK diagram and associated histogram of the distribution within the different compound classes of **c** common compounds to all $WEOM_{SPE}$ samples, **d** compounds only detected in lichens $WEOM_{SPE}$, **e** compounds only detected in *E. vaginatum* $WEOM_{SPE}$, **f** compounds only detected in *Betula* $WEOM_{SPE}$ and **g** compounds only detected in *Salix sp.* $WEOM_{SPE}$ **h** compounds only detected in lichen ("L") $WEOM_{SPE}$ (red), and compounds only detected in vascular plants ("V") $WEOM_{SPE}$ (green), **i** compounds only detected in lichen ("L") $WEOM_{SPE}$ (red), compounds only detected in graminoids ("G") $WEOM_{SPE}$ (yellow), and compounds only detected in trees and shrub ("T + S") $WEOM_{SPE}$ (blue-green)

3D Fluorescence spectroscopy

For *C. stellaris*, *F. nivalis*, *B. nana*, and *B. pubescens* WEOM, the maximum fluorescence intensity was observed at $(Em_{max}/Ex_{max}) = (275/300–310)$, representing the tyrosine-like material. It was also present in 1 of the 3 *Salix* sp. WEOM, the two others having their maximum fluorescence intensity at $(Em_{max}/Ex_{max}) = (270/292)$ (Fig. SI3). *E. vaginatum* WEOM were the only ones having a local maximum fluorescence intensity at $(Em_{max}/Ex_{max}) = (275/329)$. Lichen WEOM had a secondary local maximum at $(Em_{max}/Ex_{max}) = (275/340–350)$, corresponding to the tryptophan-like components. All WEOM had a local maximum fluorescence intensity at $(Em_{max}/Ex_{max}) = (300–340/410–450)$, corresponding to the humic-like compounds.

BIX (positively correlated to the relative proportion of fresh biological products vs. terrestrial contribution to DOM, Table 2) and FI (positively correlated to the relative proportion of microbial derived vs. higher plant derived OM to the DOM pool, Table 2) values ranged between 0.16 and 0.79, and 0.95 and 1.60 respectively (Table 4), but were not significantly different between vascular plants and lichens WEOM. Individual HIX (positively correlated with humification and aromatic, Table 2) values ranged between 0.05 and 0.59, and were significantly higher for lichen WEOM compared to vascular plant WEOM (Table 4).

High resolution mass spectrometry of $WEOM_{SPE}$ samples

Molecular diversity of $WEOM_{SPE}$ through ESI(−)

The ESI(−) HRMS full scan mass spectra of the two lichen and five vascular plant $WEOM_{SPE}$ samples are displayed in fig. SI4, and the information of each $WEOM_{SPE}$ sample (parameters, and proxies) are summarized in SI5. All *m/z* peaks were observed in the 50–450 mass range, with each $WEOM_{SPE}$ sample displaying distinct molecular features. Lichens displayed a higher molecular diversity compared to vascular plants: the number of unique monoisotopic peaks detected ranged between 679 and 781 for lichen $WEOM_{SPE}$ samples and between 259 and 682 for vascular plants (SI6).

It is noteworthy that for each comparison, a great number of detected compounds are common to lichens, graminoids, and shrubs and trees respectively. Lichen $WEOM_{SPE}$ samples had 596 compounds in common (Fig. SI6-a), which represented 69% of the detected compounds in lichens. Concerning *E. vaginatum* $WEOM_{SPE}$ samples, 374 molecules were common to (Jun.) and (Sep.) samples, which represented 56% of the detected compounds in *E. vaginatum* $WEOM_{SPE}$ samples. Similarly, *B. nana*, *B. pubescens*, and *Salix* sp. $WEOM_{SPE}$ samples had 171 common compounds, representing 21% of the total detected compounds. *B. nana* and *B. pubescens* $WEOM_{SPE}$ samples had a total of 454 (283 + 171) common compounds, representing 57% of the total detected compounds in shrubs and trees $WEOM_{SPE}$.

Among all molecules detected in the $WEOM_{SPE}$ of the 4 groups of vegetation (Fig. 4a), a total of 117 molecules were common to all samples, representing 15% of the detected compounds. On the other hand, 159, 36, 27, and 72 molecular features were specific to lichen, *Salix* sp., *E. vaginatum*, and *Betula* $WEOM_{SPE}$ samples respectively. The Venn diagram also enabled to highlight 159 and 16 specific compounds in lichen and vascular plant $WEOM_{SPE}$ samples respectively. Graminoids $WEOM_{SPE}$ samples displayed 27 specific compounds, compared to 18 for shrubs and trees.

Elemental ratios and Van Krevelen diagrams

Based on the VK diagram, the 117 common detected compounds to all $WEOM_{SPE}$ samples were largely lignin-like, and protein-like and lipid-like compounds, and a few were amino sugar-like and carbohydrate compounds (Fig. 4b, c).

The positioning of specific compounds on VK diagrams was different between lichens, *E. vaginatum, Betula*, and *Salix* sp. $WEOM_{SPE}$ samples (Fig. 4d–g respectively), as illustrated by the histograms of biomolecule family proportions. For all samples, the largest biomolecule family is the lignin-like, however, the proportion of others is specific: A great proportion of the compounds specific to lichen $WEOM_{SPE}$ corresponded to protein-like, lipid-like, and unsaturated HC (compared to other samples), whereas few corresponded to aromatic structures, and tannin-like compounds (Fig. 4d). On the other hand, apart from lignin-like compounds, *E. vaginatum* $WEOM_{SPE}$ specific compounds were dispersed on the VK diagram, and likely corresponded to protein-like and amino sugar like and carbohydrates (Fig. 3e), whereas no unsaturated HC nor aromatic structure were detected. Besides lignin-like compounds, the VK diagram of *Betula* $WEOM_{SPE}$ specific compounds related to an important proportion of protein-like, aromatic structures, and tannin-like compounds. (Fig. 4f). *Salix* sp. $WEOM_{SPE}$ specific compounds included a great proportion of specific compounds corresponding to amino sugar-like and carbohydrates, aromatic structures, and tannin-like compounds (Fig. 4g).

It is noteworthy that lichen specific compounds had low O/C (mean 0.38), compared to vascular plants (mean 0.59) which had common compounds mostly in lignin-like compounds, and amino sugar-like and carbohydrates (Fig. 4h). Within vascular plants, *E. vaginatum* samples had specific compounds with lower O/C (mean 0.42) compared to trees and shrubs compounds (mean 0.73) which had mostly amino sugar-like and carbohydrates like compounds in common (Fig. 4i). In contrast, the H/C of specific compounds did not vary between lichen and vascular plant $WEOM_{SPE}$ specific compounds (respectively 1.37 and 1.43).

Discussion

Relationship between vegetation OM and WEOM properties

Extractability of C and N

The C/N ratios were either higher than DOC/DN (*C. stellaris*, *F. nivalis*, and *E. vaginatum*), lower than DOC/DN (*B. nana*), or equal to DOC/DN (*B. pubescens* and *Salix* sp.) (Fig. 2). The comparison between C/N and DOC/DN enabled to discuss C and N relative extractability: a lower DOC/DN compared to C/N implies a greater extractability of N relatively to C. Consequently, N appears more extractable than C in lichens and *E. vaginatum*; C appeared more extractable than N in *B. nana*; and C was as extractable as N in *B. pubescens* and *Salix* sp. samples. It seemed that relative extractability of C and N differed between PFT as highlighted by specific trends identified to lichens, graminoids, and trees and shrubs, respectively (Fig. 2).

It is noteworthy that the relative extractability varies between genus (*Betula* vs. *Salix.*) and also between young leaves (buds) of *B. pubescens* or *Salix* sp. and the mature leaves of *B. nana*. The relative extractability of C and N also varies, due to multiple factors that control the C and N form in leaves (Chapin et al. 1986; Güsewell 2004; Lambers et al. 2008), such as water and nutrient supply (Weih et al. 2011), age of the vegetation (Hu et al. 2018), leaf maturity (Aerts et al. 2012), light interception (Evans 1989), and seasonality (Chapin et al. 1986). As snow can appear from September in arctic environments (Andresen et al. 2018), vegetation begins to senesce in August to avoid the loss of resources (Andresen et al. 2018; Parker et al. 2021) which can result in a shift of C/N between July and September (Westergaard-Nielsen 2021). The differences between the elementary composition measured in this study and the literature (Czimczik et al. 2003; Ellis et al. 2003; Tretiach et al. 2007; Aerts et al. 2009; Wang and Moore 2014) can also be attributed to these factors.

Extractability vs. hydrophobicity of compound classes

Despite not quantitative, results obtained through ^{13}C NMR and HRMS (Figs. 3, 4) highlighted the diversity

of molecular composition of WEOM from different species and showed consistent composition with the biochemistry of lichens, trees, and shrubs (Kögel-Knabner 2002; Storeheier et al. 2002; Raven et al. 2006; Brady and Weil 2008). Therefore, our results tended to show that the composition of WEOM was directly related to the vegetation OM composition, invalidating the hypothesis of a homogeneous production of DOM (as opposed to vegetation specific) during the leaching process. In contrary, the vegetation leachates might thus be as diverse as initial vegetation OM.

Indeed, NMR spectra of vegetation OM were specific to vegetation sources, and those specificities were also observed in WEOM samples: all vegetation OM sample spectra showed the presence of lipids, polysaccharides, and amino-acids. Spectra of the present study clearly reflected the contribution of lignin in vascular plants, and consistently, not in lichens. Condensed tannins, which were also phenolic compounds, might be present in vascular plants. Those observations were consistent with previous studies on similar PFT (Preston and Trofymow 2000; Kögel-Knabner 2002; Storeheier et al. 2002; Czimczik et al. 2003; Raven et al. 2006; Brady and Weil 2008; Moody et al. 2018; Parker et al. 2018). The *E. vaginatum* WEOM showed a singular NMR spectrum that reflected the presence of amino-acids (namely alanine, arginine, asparagine, aspartic acid, glutamic acid, methionine, and phenylalanine) (Stothers 2012). Accordingly, Chapin et al. (1986) mentioned the first five cited above as the major amino acids of *E. vaginatum* stem, despite seasonal variations. Despite the latter being clearly detected in this sample, differential absorbance of water by WEOM molecules may have strongly increase the contribution of some hydrophilic compounds (Knicker 2011), especially the high contribution of very thin peaks at 35 and 52 ppm and in the carboxylic C region are suspected to reflect the effect of this water uptake.

Interestingly, the species with the highest aromatic C content in vegetation OM (namely *Betula* and *Salix* samples), were the most extractable samples (Table 3). The aromatic C and alkyl C relative high contributions (not quantified) were observed in NMR spectra of WEOM samples despite being considered to reflect the hydrophobic compounds contribution, whereas the O-alkyl and carbonyl C reflecting the hydrophilic part of OM (Monda et al. 2017) were

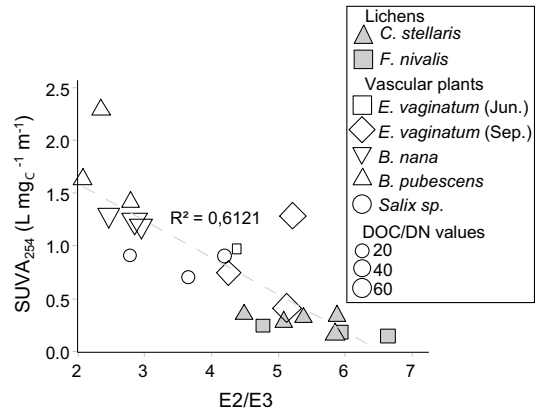

Fig. 5 Relationship between E2/E3 and $SUVA_{254}$ (L mgC^{-1} m^{-1}) of plant WEOM. Form of the dots refers to the species, and color to vascular and non-vascular samples: *C. stellaris* (solid triangle), *F. nivalis* (solid square), *E. vaginatum* (blank triangle), *B. nana* (blank diamond), *B. pubescens* (blank square), and *Salix* sp. (blank circle). Size of the dots is related to DOC/DN values of WEOM. Each point represents one sample. The linear regression line and equation are for vascular plants and lichen samples

expected to be of greater contribution. These conclusions are contradictory to Fu et al. (2019) study, which demonstrated a positive correlation between aromatic C content in (NOM) and its hydrophobicity. This counterintuitive high contribution of hydrophobic compounds to DOM, confirmed with $SUVA_{254}$ and a_{350} values, was previously highlighted in WEOM from lake sediments (Li et al. 2014).

Properties and potential degradability of WEOM from different species

The contribution of long chain aliphatic and complex aromatic (condensed HC, lignin-like and tannin-like) compounds to the WEOM samples illustrates the relative recalcitrancy of some molecules in the vegetation leachates. However, vegetation fluorescence spectra were largely dominated by tyrosine-like and tryptophan-like compounds, which highlighted the high contribution of labile C pool (e.g., low molecular weight organic compounds, carbohydrates, amino sugars), that tends to be degraded preferentially by microorganisms (Herbert and Bertsch 1995). This contribution of labile C pool to DOM has already been reported in previous studies of leaf, and leaf litter leachates (Wheeler et al. 2017; Garcia et al. 2018;

D'Andrilli et al. 2019), and are expected to decrease during DOM degradation (Don and Kalbitz 2005; Hunt and Ohno 2007; D'Andrilli et al. 2019).

However, it is possible to compare the biodegradability of WEOM produced by different vegetation. As highlighted by the VK diagrams, a non-negligible proportion of the specific compounds of lichens $WEOM_{SPE}$ were lipid-like, protein-like, and amino sugar-like/carbohydrate compounds with high potential degradability, whereas vascular plants $WEOM_{SPE}$ samples had more lignin-like and tannins-like compounds, which are of greater recalcitrancy. A differential degradability could also be expected for *E. vaginatum* and shrub and trees, as *E. vaginatum* had a greater proportion of protein-like and lignin-like compounds, and few aromatic structures and tannin-like compounds compared to trees and shrubs. Furthermore, the $SUVA_{254}$, E2/E3, and DOC/DN are statistically different between lichens and vascular plants, and are indirectly related to the potential stability of WEOM. As illustrated in Fig. 5, the combination of these information revealed a positive correlation between aromaticity and molecular weight of vegetation WEOM. It enabled to strongly discriminate lichens from vascular plants based on multiple proxies and all converge towards the same conclusion: the lichens produce DOM with a biodegradability likely higher than DOM originating from vascular plants. Moreover, the degradability of graminoids DOM is in between. This underlines that the molecular composition of WEOM from different PFT is an important parameter that may strongly influence its fate and its degradability (Herbert and Bertsch 1995; Kiikkilä et al. 2006; Bonanomi et al. 2013).

Implication for Arctic studies

Use of spectroscopic proxies for plant leachate and DOM characterization in Arctic environments

The DOM sources and level of microbial processing is usually of great interest to trace environmental changes and effects of climate change. The characterization of the unprocessed vegetation WEOM through classical spectroscopy indices was thus confronted to the literature data of DOM from Arctic environments. Then, optical and molecular indices were compared to discuss the validity of using them for fresh vegetation leachate studies.

It has previously been reported that $SUVA_{254}$ of leaf and soil leachates (soils, permafrost, and active layers) ranged from 0.4 to 2.3 L mg_C^{-1} m^{-1}, and 1.2 to 3.8 L mg_C^{-1} m^{-1} respectively. $SUVA_{254}$ of rivers and fjords ranged from 0.03 to 8.24 L mg_C^{-1} m^{-1}, and 1.54 to 2.86 L mg_C^{-1} m^{-1}, respectively, with important spatial and seasonal variations (Wickland et al. 2007, 2018; Mann et al. 2012, 2016; Fouché et al. 2017, 2020; Mangal et al. 2020; McGovern et al. 2020; Beel et al. 2021). HIX values of soils and rivers were reported to range between 0.65 and 0.95, and between 0.13 and 0.99, respectively (Fouché et al. 2017; Wickland et al. 2018). The comparison of values from several studies highlights the difficulties to differentiate one environment from another based on aromaticity indices, especially when considering spatial and seasonal variations. Furthermore, the HIX and $SUVA_{254}$, were expected to be positively correlated, as they were both reported to be positively correlated with aromaticity (See Table 2, Ohno 2002; Weishaar et al. 2003; Ohno et Bro 2006), but the results of the current study show a negative correlation between $SUVA_{254}$ and HIX in fresh vegetation leachates. This is due to the HIX index inconsistently reflecting a significantly higher aromaticity for lichens compared to vascular plants, whereas $SUVA_{254}$ of lichens appear slightly below the $SUVA_{254}$ of vascular plants, likely due to the low phenolic and aromatic moieties, as revealed by the ^{13}C-NMR data (Fig. 3). Hence, the latter results suggest that the HIX index should not be used to compare the compositions of primary DOM sources, i.e., fresh vegetation WEOM that have not been exposed to any humification processes yet.

The comparison of optical and molecular indices indicates that neither $SUVA_{254}$ nor HIX (both aromaticity proxies) are significantly correlated to the proportion of aromatic structure, the mean AI, or the proportion of condensed aromatic structure ($AI > 0.67$) in a sample (Fig. 6). However, the HIX is significantly correlated to the proportion of compounds with olefinic/alicyclic compounds ($0 < AI \leq 0.5$), whereas the $SUVA_{254}$ is significantly negatively correlated to the relative proportion of lipid-like compounds, which might reflect the high proportion of aliphatic molecules of vegetation OM. These results highlight that molecular and optical features indicate different information towards the aromaticity of a sample.

Fig. 6 Correlogram of Spearman correlations between optical indices (namely $SUVA_{254}$, HIX, S_R, E2/E3, a_{350}, FI, and BIX) and molecular proxies (proportion of lipid-like, protein-like, amino sugars and carbohydrates, unsaturated HC, lignin-like, tannin-like, and aromatic compounds, number of attributed formulae, mean O/C, mean H/C, mean DBE_{AI}, mean AI, proportions of AI = 0, proportions of AI ranging between 0 and 0.5, proportions of AI ranging between 0.5 and 0.67, and proportions of AI superior to 0.67). The color of the squares refers to sign of the correlation, and the values in the squares correspond to the p-value of the correlation (bold if significant)

In previous studies, the FI was reported to be between 1.30 and 1.7 for rivers, between 1.17 and 1.65 for permafrost leachates, and between 1.30 and 1.80 for sea water (Mann et al. 2012; Olefeldt and Roulet 2012; Wickland et al. 2018; Fouché et al. 2017, 2020; Beel et al. 2021). On the other hand, a_{350} was reported to range between 0.02 and 3.41 L mg_C^{-1} m^{-1} for river samples, and between 1.21 and 3.69 L mg_C^{-1} m^{-1} for soil leachate samples (Fouché et al. 2020; Beel et al. 2021). This highlights that neither FI nor a_{350} significantly fluctuate from a natural environment to another. Furthermore, no difference between vegetation WEOM from the present study and DOM of natural environments (soil, permafrost or rivers) from literature could be observed based on FI and a_{350} values, despite differences being expected as a reflection of vegetation freshness. Furthermore, the FI values calculated here, do not demonstrate any difference between lichen and vascular plant WEOM, whereas a_{350} clearly discriminates lichens (low phenol contribution) from vascular plants (higher phenol contribution). This result questions the use of both FI and a_{350} indices as relevant polyphenol proxies for fresh vegetation DOM characterization. Based on the comparison with the molecular indices (Fig. 6), the a_{350} and FI (positively and negatively correlated to the terrestrial plant sources) are not significantly correlated to the proportions of lignin-like or tannin-like compounds. However, the a_{350} is significantly negatively correlated to the proportion of lipid-like compounds.

The S_R index was reported to range between 0.73 and 1.32 for soil leachates, between 0.05 and 1.1 for rivers, between 1.3 and 5 for fjords, and between 0.72 and 1.9 for marine samples, with seasonal and geographical variations too (Mann et al. 2012, 2016; Drozdova et al. 2017; Fouché et al. 2017, 2020; Chen et al. 2003; Wickland et al. 2018; McGovern et al. 2020; Beel et al. 2021). The E2/E3 ratio of leaf leachates ranged from 3.2 to 6.9, from 2.8 to 5.8 for soil leachates, from 3.1 to 13.3 for estuaries, and from 3.4 to 5.8 for lakes (Mangal et al. 2020; Lei et al. 2019; Meingast et al. 2020). The freshness of the vegetation WEOM studied in here was expected to result in a significantly higher molecular weight compared to DOM collected in different natural environments. This is in accordance with the $S_R < 1.3$ measured for the different vegetation WEOM which highlights a higher molecular weight of fresh vegetation WEOM as compared to the likely more processed DOM encountered in other environments such as permafrost, rivers or marine environments. Conversely, the E2/E3 values, that discriminates lichen from vascular plant molecular weights, are consistent with leaf DOM (Meingast et al. 2020), but does not seem to distinguish fresh leaf DOM from soil or aquatic system. Furthermore, E2/E3 and S_R are not correlated, which induces that at least one of them is not a valid indicator of DOM molecular weight. The fact that S_R does not enable to discriminate PFT, whereas E2/E3 does, suggests that the use of S_R is not suitable for fresh vegetation WEOM studies. Lastly despite being both considered as molecular weight proxies, neither S_R nor E2/E3 is significantly correlated to the molecular weight calculated based on molecular information (Fig. 6).

The BIX was previously reported to correlate to the relative proportion of fresh production of DOM due to biological activity. In literature, BIX was reported to be between 0.30 to 0.80 for leaf leachates, between 0.31 and 0.63 for soil leachates, between 0.45 and 0.78 for river waters, and between 0.90 and 1.20 for sea waters (Hodgkins et al. 2016; Fouché et al. 2017, 2020; Chen et al. 2003; Meingast et al. 2020; Beel et al. 2021), in line with the reported threshold values of low, intermediate, and strong aquatic bacterial DOM (Huguet et al. 2009). The BIX ratios of vegetation WEOM calculated here are not significantly different between PFT. Furthermore, the values of vegetation WEOM (between 0.2 and 0.8) are not significantly different between lichens and vascular plants, and fall into the ranges of low and intermediate aquatic bacterial contribution categories. However, they should only be in the "low aquatic bacterial contribution" category, given the low to absent influence of bacterial contribution to these samples. At last, the BIX is not significantly correlated to any molecular indices (Fig. 6), such as the proportion of protein-like compounds, or inversely correlated to the proportion of tannin-like or lignin-like compounds.

According to these findings, the relevance of these indices to the study of unprocessed vegetation WEOM can be questioned, as illustrated by the lack of differences between WEOM vegetation sources, observed for S_R, BIX, HIX and FI (see Table 4). Furthermore, the comparison of different natural environments (as well as the fresh vegetation WEOM) also questions the relevance of the inter-study comparison

of these proxies. Considering the variability of the WEOM properties depending on the OM source (shown in this study) as well as the variety of the sampling methodologies used in the literature (such as filtration thresholds, sample storage conditions and pre-treatments required for different analytical methods), the use of this type of proxies has to be taken with a lot of caution for inter-study comparison. At last, the comparison of proxies determined through different analytical methods provides information that seems contradictory, but they actually focus on different fractions of the WEOM; optical features focus on the colored DOM, whereas HRMS Orbitrap focuses on the polar compounds. These methods are complementary, and give a more comprehensive overview of the DOM, however, the above-mentioned limits regarding the use of these measurements should always be considered to ensure correct and relevant study of DOM.

Consequences on C cycle in Arctic environment

Molecular composition, spectroscopic measurements and DOC/DN ratios enabled to discuss WEOM biodegradability, however, the use of more than one proxy (e.g., $SUVA_{254}$, E2/E3, and DOC/DN, see Fig. 5) seemed necessary in order to make reliable comparison and have a general idea of WEOM degradability potential. According to these results and proxies, lichen WEOM would be composed of low molecular weight compounds and would have low aromatic and recalcitrant compounds whereas vascular plant WEOM would contain higher molecular weight, aromatic compounds, tannins and lignins, suggesting more labile WEOM in lichens and more recalcitrant WEOM for vascular plants, especially trees and shrubs. Vegetation appears to produce variable but great amount of DOC (up to 101.9 mg_{DOC} g_{DM}^{-1}): quantity of leached DOC varies between PFT and might be higher in forests composed of trees and shrubs, compared to bogs with herbaceous, lichens and moss vegetation. Our results show that the initial WEOM produced by vegetation leaching may be as diverse as the vegetation OM from different species. Although that this initial DOM may rapidly be homogenized by microbial decomposition (Jaffé et al. 2004; Osterholz et al. 2014), numerous studies highlighted the importance of vegetation control on DOC concentration and fluxes (Neff and Hooper 2002; Ward et al. 2009; Robroek et al. 2015; Surey et al. 2020) as well as the role of the low-molecular-weight and highly-labile dissolved organic matter for C dynamics and CO_2 emissions by soils (Hees et al. 2005). We thus make the hypothesis that the changes in vegetation composition presently induced by climate changes may greatly affect the composition of DOM initially produced by vegetation leaching and might also influence related biogeochemical cycles (Neff and Hooper 2002; Malmer et al. 2005; Robroek et al. 2015, 2016). Furthermore, in Arctic ecosystem, distinctive DOC in permafrost have been reported (Fouché et al. 2020), with optical properties (fluorescence, $SUVA_{254}$, S_R, FI and a_{350}) indicating many resemblances with vegetation WEOM of this study (like great proportions of unstable tyrosine-like and tryptophan-like compounds), probably due to low temperatures that maintain permafrost frozen, and preserve DOM from degradation. Furthermore, numerous papers have highlighted the release of labile DOM following permafrost thaw (Mueller et al. 2015; Woods et al. 2011; Abbott et al. 2014; Fouché et al. 2017), which suggests that chemical properties are preserved in Arctic soils. This underlines the importance of chemical characterization of WEOM freshly produced, as these properties might also be preserved in permafrost.

Characterizing WEOM from vegetation enables to determine its extractability, thus what could reach soil then permafrost, but also to discuss its potential biodegradation in soils. Since Arctic DOM is highly sensitive to microbial degradation, its ex-situ characterization is challenging. It is well known that each specific extraction procedure affects composition and quantity of WEOM (Zsolnay 2003; Chantigny et al. 2014; Guigue et al. 2014), and results of this study may partly be an artefact of the water-extraction methodology. However, despite this potential bias, authors highlighted that the main characteristics of extracted OM proved to show relatively common features whatever the extraction procedure, especially considering no influence of soil interactions (Guigue et al. 2014) and the application of similar extraction procedure still allows comparing the properties of vegetation species in the present study. In this work, the characterization of WEOM offered great potential to characterize delicate unprocessed organic fractions, and this approach may also be suitable for permafrost sample characterization, to track

tenuous process differences between environments. According to multiple analyses, it appears that, except from *E. vaginatum*, WEOM produced by vascular plants might be less sensitive to biodegradation than WEOM produced by lichens, and among vascular plants, *E. vaginatum* WEOM might be more sensitive to biodegradation than WEOM produced by trees and shrubs. Moreover, as discussed previously, numerous environmental parameters and properties of chemical compounds influence DOM path, and using an accurate sampling method along DOM degradation continuum, or the development of a laboratory-based biodegradation monitoring experiment are necessary to confirm the conclusions made in the current study.

Conclusion

In this work, based on a multi-analysis approach, we finely characterized the WEOM specific composition and properties of different Arctic vegetation sources. Furthermore, this study enabled to highlight that WEOM composition significantly differed between vegetation sources and specifically between PFT (e.g., comparison between lichens, graminoids, and trees and shrubs). Also based on these results, vascular plants appeared to produce more WEOM compared to lichens, and WEOM from *E. vaginatum* sources appeared more degradable than trees and shrubs WEOM, but less degradable than WEOM produced by lichens. Thus, the ongoing changes of vegetation in Arctic and subarctic regions may greatly affect the composition of DOM that enters the soil and the hydrosystems as well as the biogeochemical processes the DOM is involved in. In addition, this work enabled to dismiss the use of several optical indices for the study of fresh vegetation WEOM.

Acknowledgements We acknowledge the main support of this project by the french national grant EC2CO- Biohefect/Ecodyn//Dril/MicrobiEen, DYNAMOET-TK, the METIS laboratory for additional support and the ENVEXX program (SU) for sampling financial support. Laurent Orgogozo is acknowledged for vegetation sampling, Mahaut Sourzac (EPOC) for 3D fluorescence measurements, Véronique Vaury (iEES-Paris) for EA measurements, Christelle Anquetil (METIS) and Baptiste Rigaud (IMPC platform of Sorbonne Université) for sample preparation and NMR analyses, Emmanuel Aubry (METIS) for sample preparation and TOC measurements and Amélie Guittet (OSU of Sorbonne Université) for sample preparation and absorbance measurements.

Author contributions Conceptualization: MR, MAA; Formal analysis and investigation: AA, MCB, YA; Writing—original draft preparation: AA, MAA, MCB; Writing—review and editing: AA, MAA, MCB, GH, YA, MR; Funding acquisition: MR, MAA; Supervision: MR.

Funding Funding was provided by Institut National des Sciences de l'Univers, Centre National de la Recherche Scientifique (EC2CO DYNAMOET-TK).

Data availability All data generated or analysed during this study are included in this published article and its supplementary information files.

Declarations

Conflict of interest The authors have no relevant financial or non-financial interests to disclose.

References

Abbott BW, Larouche JR, Jones JB et al (2014) Elevated dissolved organic carbon biodegradability from thawing and collapsing permafrost. J Geophys Res Biogeosci 119:2049–2063. https://doi.org/10.1002/2014JG002678

Aerts R, Callaghan TV, Dorrepaal E et al (2009) Seasonal climate manipulations result in species-specific changes in leaf nutrient levels and isotopic composition in a subarctic bog. Funct Ecol 23:680–688. https://doi.org/10.1111/j.1365-2435.2009.01566.x

Aerts R, van Bodegom PM, Cornelissen JHC (2012) Litter stoichiometric traits of plant species of high-latitude ecosystems show high responsiveness to global change without causing strong variation in litter decomposition. New Phytol 196:181–188. https://doi.org/10.1111/j.1469-8137.2012.04256.x

Agnan Y, Courault R, Alexis MA et al (2019) Distribution of trace and major elements in subarctic ecosystem soils: Sources and influence of vegetation. Sci Total Environ 682:650–662. https://doi.org/10.1016/j.scitotenv.2019.05.178

Alvarez-Rivera G, Ballesteros-Vivas D, Parada-Alfonso F et al (2019) Recent applications of high resolution mass spectrometry for the characterization of plant natural products. TrAC Trends Anal Chem 112:87–101. https://doi.org/10.1016/j.trac.2019.01.002

Andresen C, Tweedie C, Lougheed V (2018) Climate and nutrient effects on Arctic wetland plant phenology observed from phenocams. Remote Sens Environ 205:46–55. https://doi.org/10.1016/j.rse.2017.11.013

Araújo E, Strawn DG, Morra M et al (2019) Association between extracted copper and dissolved organic matter in dairy-manure amended soils. Environ Pollut 246:1020–1026. https://doi.org/10.1016/j.envpol.2018.12.070

Battin TJ (1998) Dissolved organic matter and its optical properties in a blackwater tributary of the upper Orinoco river, Venezuela. Org Geochem 28:561–569. https://doi.org/10.1016/S0146-6380(98)00028-X

Beel CR, Heslop JK, Orwin JF et al (2021) Emerging dominance of summer rainfall driving High Arctic terrestrial-aquatic connectivity. Nat Commun 12:1–9. https://doi.org/10.1038/s41467-021-21759-3

Bolan NS, Adriano DC, Kunhikrishnan A et al (2011) Dissolved organic matter. Biogeochemistry, dynamics, and environmental significance in soils, 1st edn. Elsevier, Amsterdam

Bonanomi G, Incerti G, Giannino F et al (2013) Litter quality assessed by solid state 13C NMR spectroscopy predicts decay rate better than C/N and Lignin/N ratios. Soil Biol Biochem 56:40–48. https://doi.org/10.1016/j.soilbio.2012.03.003

Bowen SR, Gregorich EG, Hopkins DW (2009) Biochemical properties and biodegradation of dissolved organic matter from soils. Biol Fertil Soils 45:733–742. https://doi.org/10.1007/s00374-009-0387-6

Brady NC, Weil RR (2008) The nature and properties of soils. Pearson, New Jersey

Chantigny MH, Harrison-Kirk T, Curtin D, Beare M (2014) Temperature and duration of extraction affect the biochemical composition of soil water-extractable organic matter. Soil Biol Biochem 75:161–166. https://doi.org/10.1016/j.soilbio.2014.04.011

Chapin FS, Shaver GR, Kedrowski RA (1986) Environmental controls over carbon, nitrogen and phosphorus fractions in eriophorum vaginatum in Alaskan Tussock Tundra. J Ecol 74:167–195

Chen J, LeBoeuf EJ, Dai S, Gu B (2003) Fluorescence spectroscopic studies of natural organic matter fractions. Chemosphere 50:639–647. https://doi.org/10.1016/S0045-6535(02)00616-1

Coble PG (1996) Characterization of marine and terrestrial DOM in seawater using excitation-emission matrix spectroscopy. Mar Chem 51:325–346. https://doi.org/10.1016/0304-4203(95)00062-3

Coble PG (2007) Marine optical biogeochemistry: the chemistry of ocean color. Chem Rev 107:402–418. https://doi.org/10.1021/cr050350+

Conte P, De Pasquale C, Novotny EH et al (2010) CPMAS 13C NMR characterization of leaves and litters from the reafforestated area of Mustigarufi in Sicily (Italy)~!2009-06-15~!2009-12-07~!2010-06-18~! Open Magn Reson J 3:89–95. https://doi.org/10.2174/1874769801003020089

Cory RM, McKnight DM (2005) Fluorescence spectroscopy reveals ubiquitous presence of oxidized and reduced quinones in dissolved organic matter. Environ Sci Technol 39:8142–8149. https://doi.org/10.1021/es0506962

Czimczik CI, Preston CM, Schmidt MWI, Schulze ED (2003) How surface fire in Siberian Scots pine forests affects soil organic carbon in the forest floor: stocks, molecular structure, and conversion to black carbon (charcoal). Glob Biogeochem Cycles. https://doi.org/10.1029/2002GB001956

D'Andrilli J, Junker JR, Smith HJ et al (2019) DOM composition alters ecosystem function during microbial processing of isolated sources. Biogeochemistry 142:281–298. https://doi.org/10.1007/s10533-018-00534-5

Dinno A (2017) dunn.test: Dunn's test of multiple comparisons using rank sums. R package version 1.3.5. https://CRAN.R-project.org/package=dunn.test

Don A, Kalbitz K (2005) Amounts and degradability of dissolved organic carbon from foliar litter at different decomposition stages. Soil Biol Biochem 37:2171–2179. https://doi.org/10.1016/j.soilbio.2005.03.019

Drozdova AN, Kravchishina MD, Khundzhua DA et al (2017) Fluorescence quantum yield of CDOM in coastal zones of the Arctic seas. Int J Remote Sens 39:9356–9379. https://doi.org/10.1080/01431161.2018.1506187

Ellis CJ, Crittenden PD, Scrimgeour CM, Ashcroft C (2003) The natural abundance of 15N in mat-forming lichens. Oecologia 136:115–123. https://doi.org/10.1007/s00442-003-1201-z

Evans JR (1989) Photosynthesis and nitrogen relationships in leaves of C3 plants. Oecologia 78:9–19. https://doi.org/10.1007/BF00377192

Fellman JB, Hood E, Spencer RGM (2010) Fluorescence spectroscopy opens new windows into dissolved organic matter dynamics in freshwater ecosystems: a review. Limnol Oceanogr 55:2452–2462. https://doi.org/10.4319/lo.2010.55.6.2452

Fouché J, Lafrenière MJ, Rutherford K, Lamoureux S (2017) Seasonal hydrology and permafrost disturbance impacts on dissolved organic matter composition in High Arctic headwater catchments. Arct Sci 3:378–405. https://doi.org/10.1139/as-2016-0031

Fouché J, Christiansen CT, Lafrenière MJ et al (2020) Canadian permafrost stores large pools of ammonium and optically distinct dissolved organic matter. Nat Commun. https://doi.org/10.1038/s41467-020-18331-w

Frey KE, Smith LC (2005) Amplified carbon release from vast West Siberian peatlands by 2100. Geophys Res Lett 32:1–4. https://doi.org/10.1029/2004GL022025

Fu H, Liu K, Alvarez PJJ et al (2019) Quantifying hydrophobicity of natural organic matter using partition coefficients in aqueous two-phase systems. Chemosphere 218:922–929. https://doi.org/10.1016/j.chemosphere.2018.11.183

Gangloff S, Stille P, Pierret MC et al (2014) Characterization and evolution of dissolved organic matter in acidic forest soil and its impact on the mobility of major and trace elements (case of the Strengbach watershed). Geochim Cosmochim Acta 130:21–41. https://doi.org/10.1016/j.gca.2013.12.033

Garcia RD, del Diéguez M, C, Gerea M, et al (2018) Characterisation and reactivity continuum of dissolved organic matter in forested headwater catchments of Andean Patagonia. Freshw Biol 63:1049–1062. https://doi.org/10.1111/fwb.13114

Grannas AM, Hockaday WC, Hatcher PG et al (2006) New revelations on the nature of organic matter in ice cores. J Geophys Res Atmos 111:1–10. https://doi.org/10.1029/2005JD006251

Gregorich EG, Liang BC, Drury CF et al (2000) Elucidation of the source and turnover of water soluble and microbial biomass carbon in agricultural soils. Soil Biol Biochem 32:581–587. https://doi.org/10.1016/S0038-0717(99)00146-7

Guigue J, Mathieu O, Lévêque J et al (2014) A comparison of extraction procedures for water-extractable organic matter in soils. Eur J Soil Sci 65:520–530. https://doi.org/10.1111/ejss.12156

Guo M, Chorover J (2003) Transport and fractionation of dissolved organic. Soil Sci 168:108–118. https://doi.org/10.1097/01.ss.0000055306.23789.65

Güsewell S (2004) N: P ratios in terrestrial plants: variation and functional significance. New Phytol 164:243–266. https://doi.org/10.1111/j.1469-8137.2004.01192.x

Helms RJ, Stubbins A, Ritchie JD et al (2008) Absorption spectral slopes and slope ratios as indicators of molecular weight, source, and photobleaching of chromophoric dissolved organic matter (Limnology and Oceanography 53 955–969). Limnol Oceanogr 54:1023. https://doi.org/10.4319/lo.2009.54.3.1023

Herbert BE, Bertsch PM (1995) Chacterization of dissolved and colloidal organical matter in soil solution: a review. Carbon forms and functions in forest. Soils. Soil Science Society of America, Madison, pp 63–88

Hodgkins SB, Tfaily MM, Podgorski DC et al (2016) Elemental composition and optical properties reveal changes in dissolved organic matter along a permafrost thaw chronosequence in a subarctic peatland. Geochim Cosmochim Acta 187:123–140. https://doi.org/10.1016/j.gca.2016.05.015

Hu YF, Shu XY, He J et al (2018) Storage of C, N, and P affected by afforestation with Salix cupularis in an alpine semiarid desert ecosystem. L Degrad Dev 29:188–198. https://doi.org/10.1002/ldr.2862

Huguet A, Vacher L, Relexans S et al (2009) Properties of fluorescent dissolved organic matter in the Gironde Estuary. Org Geochem 40:706–719. https://doi.org/10.1016/j.orggeochem.2009.03.002

Hunt JF, Ohno T (2007) Characterization of fresh and decomposed dissolved organic matter using excitation-emission matrix fluorescence spectroscopy and multiway analysis. J Agric Food Chem 55:2121–2128. https://doi.org/10.1021/jf063336m

Jaffé R, Boyer JN, Lu X et al (2004) Source characterization of dissolved organic matter in a subtropical mangrove-dominated estuary by fluorescence analysis. Mar Chem 84:195–210. https://doi.org/10.1016/j.marchem.2003.08.001

Jassey VEJ, Reczuga MK, Zielińska M et al (2018) Tipping point in plant–fungal interactions under severe drought causes abrupt rise in peatland ecosystem respiration. Glob Chang Biol 24:972–986. https://doi.org/10.1111/gcb.13928

Johnston SE, Bogard MJ, Rogers JA et al (2019) Constraining dissolved organic matter sources and temporal variability in a model sub-Arctic lake. Biogeochemistry 146:271–292. https://doi.org/10.1007/s10533-019-00619-9

Kaiser K, Canedo-Oropeza M, McMahon R, Amon RMW (2017) Origins and transformations of dissolved organic matter in large Arctic rivers. Sci Rep 7:1–11. https://doi.org/10.1038/s41598-017-12729-1

Kiikkilä O, Kitunen V, Smolander A (2005) Degradability of dissolved soil organic carbon and nitrogen in relation to tree species. FEMS Microbiol Ecol 53:33–40. https://doi.org/10.1016/j.femsec.2004.08.011

Kiikkilä O, Kitunen V, Smolander A (2006) Dissolved soil organic matter from surface organic horizons under birch and conifers: degradation in relation to chemical characteristics. Soil Biol Biochem 38:737–746. https://doi.org/10.1016/j.soilbio.2005.06.024

Kim S, Kramer RW, Hatcher PG (2003) Graphical method for analysis of ultrahigh-resolution broadband mass spectra of natural organic matter, the Van Krevelen diagram. Anal Chem 75:5336–5344

Knicker H (2011) Solid state CPMAS 13C and 15N NMR spectroscopy in organic geochemistry and how spin dynamics can either aggravate or improve spectra interpretation. Org Geochem 42:867–890. https://doi.org/10.1016/j.orggeochem.2011.06.019

Koch BP, Dittmar T (2006) From mass to structure : an aromaticity index for high-resolution mass data of natural organic matter. Rapid Commun Mass Spectrom 20:926–932. https://doi.org/10.1002/rcm.7433

Kögel-Knabner I (1997) 13C and 15N NMR spectroscopy as a tool in soil organic matter studies. Geoderma 80:243–270. https://doi.org/10.1016/S0016-7061(97)00055-4

Kögel-Knabner I (2002) The macromolecular organic composition of plant and microbial residues as inputs to soil organic matter. Soil Biol Biochem 34:139–162

Kögel-Knabner I (2017) The macromolecular organic composition of plant and microbial residues as inputs to soil organic matter: fourteen years on. Soil Biol Biochem 105:A3–A8. https://doi.org/10.1016/j.soilbio.2016.08.011

Lambers H, Chapin FS, Pons TL et al (2008) Plant water relations. Springer, New York

Lei X, Pan J, Devlin AT (2019) Characteristics of absorption spectra of chromophoric dissolved organic matter in the Pearl River Estuary in spring. Remote Sens. https://doi.org/10.3390/rs11131533

Li Y, Wang S, Zhang L et al (2014) Composition and spectroscopic characteristics of dissolved organic matter extracted from the sediment of Erhai Lake in China. J Soils Sedim 14:1599–1611. https://doi.org/10.1007/s11368-014-0916-2

Liu F, Wang D, Zhang B, Huang J (2021) Concentration and biodegradability of dissolved organic carbon derived from soils: a global perspective. Sci Total Environ 754:142378. https://doi.org/10.1016/j.scitotenv.2020.142378

Lynch LM, Machmuller MB, Boot CM et al (2019) Dissolved organic matter chemistry and transport along an Arctic Tundra Hillslope. Glob Biogeochem Cycles 33:47–62. https://doi.org/10.1029/2018GB006030

Malmer N, Johansson T, Olsrud M et al (2005) Vegetation, climatic changes and net carbon sequestration in a North-Scandinavian subarctic mire over 30 years. Glob Change Biol 11:1895–1909. https://doi.org/10.1111/j.1365-2486.2005.01042.x

Mangal V, DeGasparro S, Beresford DV, Guéguen C (2020) Linking molecular and optical properties of dissolved organic matter across a soil-water interface on Akimiski Island (Nunavut, Canada). Sci Total Environ 704:135415. https://doi.org/10.1016/j.scitotenv.2019.135415

Mann PJ, Davydova A, Zimov N et al (2012) Controls on the composition and lability of dissolved organic matter in Siberia's Kolyma River basin. J Geophys Res Biogeosciences 117:1–15. https://doi.org/10.1029/2011JG001798

Mann PJ, Spencer RGM, Hernes PJ et al (2016) Pan-arctic trends in terrestrial dissolved organic matter from optical

measurements. Front Earth Sci 4:1–18. https://doi.org/10.3389/feart.2016.00025

Maria E, Crançon P, Lespes G, Bridoux MC (2019) Spatial variation in the molecular composition of dissolved organic matter from the Podzol soils of a temperate pine forest. ACS Earth Space Chem 3:1685–1696. https://doi.org/10.1021/acsearthspacechem.9b00164

Massiot D, Fayon F, Capron M et al (2002) Modelling one- and two-dimensional solid-state NMR spectra. Magn Reson Chem 40:70–76. https://doi.org/10.1002/mrc.984

McGovern M, Pavlov AK, Deininger A et al (2020) Terrestrial Inputs drive seasonality in organic matter and nutrient biogeochemistry in a high arctic Fjord System (Isfjorden, Svalbard). Front Mar Sci 7:1–15. https://doi.org/10.3389/fmars.2020.542563

McKnight DM, Boyer EW, Westerhoff PK et al (2001) Spectrofluorometric characterization of dissolved organic matter for indication of precursor organic material and aromaticity. Limnol Oceanogr 46:38–48. https://doi.org/10.4319/lo.2001.46.1.0038

Meingast KM, Grunert BK, Green SA et al (2020) Insights on dissolved organic matter production revealed by removal of charge-transfer interactions in senescent leaf leachates. Water (switzerland). https://doi.org/10.3390/W12092356

Minor EC, Swenson MM, Mattson BM, Oyler AR (2014) Structural characterization of dissolved organic matter: a review of current techniques for isolation and analysis. Environ Sci Process Impacts 16:2064–2079. https://doi.org/10.1039/c4em00062e

Monda H, Cozzolino V, Vinci G et al (2017) Molecular characteristics of water-extractable organic matter from different composted biomasses and their effects on seed germination and early growth of maize. Sci Total Environ 590–591:40–49. https://doi.org/10.1016/j.scitotenv.2017.03.026

Moody CS, Worrall F, Clay GD et al (2018) A molecular budget for a peatland based upon 13C solid-state nuclear magnetic resonance. J Geophys Res Biogeosci 123:547–560. https://doi.org/10.1002/2017JG004312

Mueller CW, Rethemeyer J, Kao-kniffin J et al (2015) Large amounts of labile organic carbon in permafrost soils of northern Alaska. Glob Chang Biol 21:2804–2817. https://doi.org/10.1111/gcb.12876

Nebbioso A, Piccolo A (2013) Molecular characterization of dissolved organic matter (DOM): a critical review. Anal Bioanal Chem 405:109–124. https://doi.org/10.1007/s00216-012-6363-2

Neff J, Hooper D (2002) Vegetation and climate controls on potential CO2, DOC and DON production in northern latitude soils. Glob Change Biol 9:872–884. https://doi.org/10.1046/j.1365-2486.2002.00517.x

Nielsen CS, Michelsen A, Strobel BW et al (2017) Correlations between substrate availability, dissolved CH4, and CH4 emissions in an arctic wetland subject to warming and plant removal. J Geophys Res Biogeosci 122:645–660. https://doi.org/10.1002/2016JG003511

O'Donnell J, Douglas T, Barker A (2021) Changing biogeochemical cycles of organic carbon, nitrogen, phosphorus, and trace elements in ARCTIC Rivers. Arctic hydrology, permafrost and ecosystems. Springer, New York, pp 315–348

Ohno T (2002) Fluorescence inner-filtering correction for determining the humification index of dissolved organic matter. Environ Sci Technol 36:742–746. https://doi.org/10.1021/es0155276

Ohno T, Bro R (2006) Dissolved organic matter characterization using multiway spectral decomposition of fluorescence landscapes. Soil Sci Soc Am J 70:2028–2037. https://doi.org/10.2136/sssaj2006.0005

Olefeldt D, Roulet NT (2012) Effects of permafrost and hydrology on the composition and transport of dissolved organic carbon in a subarctic peatland complex. J Geophys Res Biogeosci 117:1–15. https://doi.org/10.1029/2011JG001819

Osterholz H, Dittmar T, Niggemann J (2014) Molecular evidence for rapid dissolved organic matter turnover in Arctic fjords. Mar Chem 160:1–10. https://doi.org/10.1016/j.marchem.2014.01.002

Pan Q, Zhuo X, He C et al (2020) Validation and evaluation of high-resolution orbitrap mass spectrometry on molecular characterization of dissolved organic matter. ACS Omega 5:5372–5379. https://doi.org/10.1021/acsomega.9b04411

Parker TC, Subke JA, Wookey PA (2015) Rapid carbon turnover beneath shrub and tree vegetation is associated with low soil carbon stocks at a subarctic treeline. Glob Chang Biol 21:2070–2081. https://doi.org/10.1111/gcb.12793

Parker TC, Sanderman J, Holden RD et al (2018) Exploring drivers of litter decomposition in a greening Arctic: results from a transplant experiment across a treeline. Ecology 99:2284–2294. https://doi.org/10.1002/ecy.2442

Parker TC, Unger S, Moody M et al (2021) Intraspecific variation in phenology offers resilience to climate change for Eriophorum vaginatum. Arct Sci 17:1–17. https://doi.org/10.1139/as-2020-0039

Parot J (2017) Développement méthodologique du fractionnement par couplage flux/force (AF4) et spectroscopie optique pour l ' étude de la matière organique dissoute aquatique : application aux estuaires de Seine et de Gironde, HAL Id : tel-0159. 355

Peacock M, Evans CD, Fenner N et al (2014) UV-visible absorbance spectroscopy as a proxy for peatland dissolved organic carbon (DOC) quantity and quality: Considerations on wavelength and absorbance degradation. Environ Sci Process Impacts 16:1445–1461. https://doi.org/10.1039/c4em00108g

Pokrovsky OS, Manasypov RM, Kopysov SG et al (2020) Impact of permafrost thaw and climate warming on riverine export fluxes of carbon, nutrients and metals in Western Siberia. Water (switzerland). https://doi.org/10.3390/w12061817

Polishchuk YM, Bogdanov AN, Polishchuk VY et al (2017) Size distribution, surface coverage, water, carbon, and metal storage of thermokarst lakes in the permafrost zone of the western Siberia lowland. Water (switzerland). https://doi.org/10.3390/w9030228

Preston CM, Trofymow JA (2000) Variability in litter quality and its relationship to litter decay in Canadian forests. Can J Bot 78:1269–1287. https://doi.org/10.1139/cjb-78-10-1269

Raven PH, Evert RF, Eichhorn SL (2006) Biologie végétale, 6th edn

Ren ZL, Tella M, Bravin MN et al (2015) Effect of dissolved organic matter composition on metal speciation in soil solutions. Chem Geol 398:61–69. https://doi.org/10.1016/j.chemgeo.2015.01.020

Robroek BJM, Jassey VEJ, Kox MAR et al (2015) Peatland vascular plant functional types affect methane dynamics by altering microbial community structure. J Ecol 103:925–934. https://doi.org/10.1111/1365-2745.12413

Robroek BJM, Albrecht RJH, Hamard S et al (2016) Peatland vascular plant functional types affect dissolved organic matter chemistry. Plant Soil 2:135–143. https://doi.org/10.1007/s11104-015-2710-3

Rosario-Ortiz FL, Korak JA (2017) Oversimplification of dissolved organic matter fluorescence analysis: potential pitfalls of current methods. Environ Sci Technol 51:759–761. https://doi.org/10.1021/acs.est.6b06133

Roth V-N, Lange M, Simon C et al (2019) Persistence of dissolved organic matter explained by molecular changes during its passage through soil. Nat Geosci 12:755–761

Schwarzenbach RP, Gschwend PM, Imboden DM (2016) Environmental organic chemistry. John Wiley, Hoboken

Storeheier PV, Mathiesen SD, Tyler NJC, Olsen MA (2002) Nutritive value of terricolous lichens for reindeer in winter. Lichenologist 34:247–257. https://doi.org/10.1006/lich.2002.0394

Stothers J (2012) Carbon-13 NMR spectroscopy: organic chemistry, a series of monographs, vol 24. Elsevier, Amsterdam

Surey R, Schimpf C, Sauheitl L et al (2020) Potential denitrification stimulated by water-soluble organic carbon from plant residues during initial decomposition. Soil Biol Biochem 147:107841. https://doi.org/10.1016/j.soilbio.2020.107841

Tretiach M, Adamo P, Bargagli R et al (2007) Lichen and moss bags as monitoring devices in urban areas. Part I: influence of exposure on sample vitality. Environ Pollut 146:380–391. https://doi.org/10.1016/j.envpol.2006.03.046

Van Hees PAW, Jones DL, Finlay R et al (2005) The carbon we do not see: the impact of low molecular weight compounds on carbon dynamics and respiration in forest soils: a review. Soil Biol Biochem 37:1–13

Wagner S, Cawley KM, Rosario-Ortis F, Jaffé R (2015) In-stream sources and links between particulateand dissolved black carbon following a wildfire. Biogeochemistry 124:145–162

Walker D (2000) Hierarchical subdivision of Artic tundra based on vegetation response to climate, parent material and topography. Glob Change Biol 6:19–34. https://doi.org/10.1046/j.1365-2486.2000.06010.x

Walvoord MA, Voss CI, Wellman TP (2012) Influence of permafrost distribution on groundwater flow in the context of climate-driven permafrost thaw : example from Yukon Flats Basin, Alaska, United States. Water Resour Res 48:1–17. https://doi.org/10.1029/2011WR011595

Wang M, Moore TR (2014) Carbon, nitrogen, phosphorus, and potassium stoichiometry in an ombrotrophic peatland reflects plant functional type. Ecosystems 17:673–684. https://doi.org/10.1007/s10021-014-9752-x

Ward SE, Bardgett RD, McNamara NP et al (2009) Plant functional group identity influences short-term peatland ecosystem carbon flux: evidence from a plant removal experiment. Funct Ecol 23:445–462. https://doi.org/10.1111/j.1365-2435.2008.01521.x

Wei T, Simko V (2021). R package 'corrplot': Visualization of a Correlation Matrix (Version 0.92). https://github.com/taiyun/corrplot

Weih M, Bonosi L, Ghelardini L, Rönnberg-Wästljung AC (2011) Optimizing nitrogen economy under drought: Increased leaf nitrogen is an acclimation to water stress in willow (Salix spp.). Ann Bot 108:1347–1353. https://doi.org/10.1093/aob/mcr227

Weishaar JL, Aiken GR, Bergamaschi BA et al (2003) Evaluation of specific ultraviolet absorbance as an indicator of the chemical composition and reactivity of dissolved organic carbon. Environ Sci Technol 37:4702–4708. https://doi.org/10.1021/es030360x

Westergaard-Nielsen A, Christiansen CT, Elberling B (2021) Growing season leaf carbon:nitrogen dynamics in Arctic tundra vegetation from ground and Sentinel-2 observations reveal reallocation timing and upscaling potential. Remote Sens Environ 262:112512. https://doi.org/10.1016/j.rse.2021.112512

Wheeler KI, Levia DF, Hudson JE (2017) Tracking senescence-induced patterns in leaf litter leachate using parallel factor analysis (PARAFAC) modeling and self-organizing maps. J Geophys Res Biogeosci 122:2233–2250. https://doi.org/10.1002/2016JG003677

Wickland KP, Neff JC, Aiken GR (2007) Dissolved organic carbon in Alaskan boreal forest: sources, chemical characteristics, and biodegradability. Ecosystems 10:1323–1340. https://doi.org/10.1007/s10021-007-9101-4

Wickland KP, Waldrop MP, Aiken GR et al (2018) Dissolved organic carbon and nitrogen release from boreal Holocene permafrost and seasonally frozen soils of Alaska. Environ Res Lett. https://doi.org/10.1088/1748-9326/aac4ad

Woods GC, Simpson MJ, Pautler BG et al (2011) Evidence for the enhanced lability of dissolved organic matter following permafrost slope disturbance in the Canadian High Arctic. Geochim Cosmochim Acta 75:7226–7241. https://doi.org/10.1016/j.gca.2011.08.013

Yates CA, Johnes PJ, Spencer RGM (2016) Assessing the drivers of dissolved organic matter export from two contrasting lowland catchments, U.K. Sci Total Environ 569–570:1330–1340. https://doi.org/10.1016/j.scitotenv.2016.06.211

Zak DR, Kling GW (2006) Microbial community composition and function across an arctic tundra landscape. Ecology 87:1659–1670. https://doi.org/10.1890/0012-9658(2006)87[1659:MCCAFA]2.0.CO;2

Zark M, Dittmar T (2018) Universal molecular structures in natural dissolved organic matter. Nat Commun 9:1–8. https://doi.org/10.1038/s41467-018-05665-9

Zsolnay Á (2003) Dissolved organic matter: Artefacts, definitions, and functions. Geoderma 113:187–209. https://doi.org/10.1016/S0016-7061(02)00361-0